AFRL-AFOSR-VA-TR-2017-0049

Superpersistent Currents in Dirac Fermion Systems

Ying Cheng Lai
ARIZONA STATE UNIVERSITY

03/06/2017
Final Report

Air Force Research Laboratory
AF Office Of Scientific Research (AFOSR)/ RTB1
Arlington, Virginia 22203
Air Force Materiel Command

REPORT DOCUMENTATION PAGE

Form Approved
OMB No. 0704-0188

1. REPORT DATE *(DD-MM-YYYY)*	2. REPORT TYPE	3. DATES COVERED *(From - To)*
07-03-2017	Final Performance	01 Dec 2015 to 30 Nov 2016

4. TITLE AND SUBTITLE
Superpersistent Currents in Dirac Fermion Systems

5a. CONTRACT NUMBER

5b. GRANT NUMBER
FA9550-15-1-0151

5c. PROGRAM ELEMENT NUMBER
61102F

6. AUTHOR(S)
Ying Cheng Lai

5d. PROJECT NUMBER

5e. TASK NUMBER

5f. WORK UNIT NUMBER

7. PERFORMING ORGANIZATION NAME(S) AND ADDRESS(ES)
ARIZONA STATE UNIVERSITY
660 S MILL AVE STE 312
TEMPE, AZ 85281 US

8. PERFORMING ORGANIZATION REPORT NUMBER

9. SPONSORING/MONITORING AGENCY NAME(S) AND ADDRESS(ES)
AF Office of Scientific Research
875 N. Randolph St. Room 3112
Arlington, VA 22203

10. SPONSOR/MONITOR'S ACRONYM(S)
AFRL/AFOSR RTB1

11. SPONSOR/MONITOR'S REPORT NUMBER(S)
AFRL-AFOSR-VA-TR-2017-0049

12. DISTRIBUTION/AVAILABILITY STATEMENT
A DISTRIBUTION UNLIMITED: PB Public Release

13. SUPPLEMENTARY NOTES

14. ABSTRACT
The principal Objective of the project was to uncover, understand, and exploit persistent currents in 2D Dirac material systems and pertinent phenomena in the emerging field of relativistic quantum nonlinear dynamics and chaos. Systematic theories and methods were developed to analyze and characterize persistent currents in these systems and their unusual physical properties. The main accomplishments are the following: (1) a physical understanding of conductance stability in chaotic and integrable graphene quantum dots with random impurities, (2) the analysis of conductance fluctuations in chaotic bilayer graphene quantum dots, (3) the identification of reverse Stark effect, anomalous optical transitions, and spin control in topological insulator quantum dots, (4) the discovery of nonlinear dynamics induced anomalous Hall effect in topological
insulators, (5) the finding that chaos can enhance spin polarization in graphene, (6) the articulation of a robust relativistic quantum two-level system, (7) the discovery and understanding of a number of novel and unusual phenomena associated with scattering of pesudospin-1 particles, (8) a proposal to resolve the paradox of breakdown of quantum-classical correspondence in optomechanics, (9) the detection of unusual level statistics in graphene billiards, (10) the unearthing of the phenomenon of superscattering of pseudospin-1 wave in a photonic lattice system, (11) the revelation of relativistic Zitterbewegung in non-Hermitian photonic systems, and (12) the elucidation of the robustness of persistent currents in two-dimensional Dirac systems in the presence of random disorders. In addition, the phenomenon of magnetic field induced flow reversal in a ferrofluidic Taylor-Couette system was uncovered, and the issues of multistability, chaos, and random signal
generation in semiconductor super lattice systems were addressed.

15. SUBJECT TERMS
Dirac fermion materials, superpersistent currents

16. SECURITY CLASSIFICATION OF:			17. LIMITATION OF ABSTRACT	18. NUMBER OF PAGES	19a. NAME OF RESPONSIBLE PERSON
a. REPORT	b. ABSTRACT	c. THIS PAGE			NACHMAN, ARJE
Unclassified	Unclassified	Unclassified	UU		19b. TELEPHONE NUMBER *(Include area code)* 703-696-8427

Standard Form 298 (Rev. 8/98)
Prescribed by ANSI Std. Z39.18

Final Report

This Final Report summarizes activities under the Air Force Office of Scientific Research (AFOSR) Grant No. FA9550-15-1-0151 entitled "Superpersistent Currents in Dirac Fermion Systems," from 1 June 2015 to 30 November 2016. PI is Ying-Cheng Lai from Arizona State University (ASU).

Contents

1 Objectives

- Objective 1 - Physical theory of superpersistent currents in Dirac fermion systems.
- Objective 2 - Superpersistent currents in graphene devices.
- Objective 3 - Effects of random disorders and maximum device size for observing superpersistent currents.
- Objective 4 - Experimental scheme to observe superpersistent currents based on topological insulators.
- Objective 5 - Application: relativistic qubit systems based on superpersistent currents.

All research Objectives have been accomplished. The results have been disseminated through refereed-journal publications and invited talks.

- Objective 1 - papers # 10 and 17 in the publication list below.
- Objective 2 - papers # 1, 2, 7, 9, and 13 in the publication list below.
- Objective 3 - paper # 17 in the publication list below.
- Objective 4 - papers # 3, 6, 11, and 14 in the publication list below.
- Objective 5 - paper # 10 in the publication list below.

The AFOSR support provided us with the opportunity to investigate a number of forefront problems beyond the original proposed research (see publication list below). In addition, *the AFOSR support helped create a new field of interdisciplinary research:* **Relativistic Quantum Chaos***, which studies the relativistic quantum manifestations of classical chaos with applications to graphene and two-dimensional Dirac material systems.*

2 List of Publications

1. G.-L. Wang, L. Ying, and Y.-C. Lai, "Conductance stability in chaotic and integrable quantum dots with random impurities," *Physical Review E* **92**, 022901, 1-10 (2015).
2. R. Bao, L. Huang, Y.-C. Lai, and C. Grebogi, "Conductance fluctuations in chaotic bilayer graphene quantum dots," *Physical Review E* **92**, 012918, 1-8 (2015).
3. H.-Y. Xu and Y.-C. Lai, "Reverse Stark effect, anomalous optical transitions, and control of spin in topological insulator quantum dots," *Physical Review B* **92**, 195120, 1-6 (2015).
4. S. Altmeyer, Y.-H. Do, and Y.-C. Lai, "Ring bursting behavior en route to turbulence in narrow gap Taylor-Couette flows," *Physical Review E* **92**, 053018, 1-10 (2015).
5. S. Altmeyer, Y.-H. Do, and Y.-C. Lai, "Magnetic field induced flow reversal in a ferrofluidic Taylor-Couette system," *Scientific Reports* **5**, 18589, 1-13 (2015).
6. G.-L. Wang, H.-Y. Xu, and Y.-C. Lai, "Nonlinear dynamics induced anomalous Hall effect in topological insulators," *Scientific Reports* **6**, 19803, 1-9 (2016).
7. L. Ying and Y.-C. Lai, " Enhancement of spin polarization by chaos in graphene quantum dot systems," *Physical Review B* **93**, 085408, 1-8 (2016).
8. L. Ying, D.-H. Huang, and Y.-C. Lai, "Multistability, chaos, and random signal generation in semiconductor superlattices," *Physical Review E* **93**, 062204, 1-9 (2016).

9. M.-K. Xu, Y.-S. Wang, R. Bao, L. Huang, and Y.-C. Lai, "Complex transport behaviors of graphene quantum dots subject to mechanical vibrations," *Europhysics Letters* **114**, 47006, 1-6 (2016).
10. H.-Y. Xu, L. Huang, and Y.-C. Lai, "A robust relativistic quantum two-level system with edge-dependent currents and spin polarization," *Europhysics Letters* **115**, 20005, 1-7 (2016).
11. H.-Y. Xu and Y.-C. Lai, "Revival resonant scattering, perfect caustics and isotropic transport of pesudospin-1 particles," *Physical Review B* **94**, 165405, 1-16 (2016).
12. G.-L. Wang, Y.-C. Lai, and C. Grebogi, "Transient chaos: breakdown of quantum-classical correspondence in optomechanics," *Scientific Reports* **6**, 35381, 1-13 (2016).
13. P. Yu, Z.-Y. Li, H.-Y. Xu, L. Huang, B. Dietz, C. Grebogi, and Y.-C. Lai, "Gaussian orthogonal ensemble statistics in graphene billiards with the shape of classically integrable billiards," *Physical Review E* **94**, 062214, 1-12 (2016).
14. H.-Y. Xu and Y.-C. Lai, "Superscattering of pseudospin-1 wave in photonic lattice," *Physical Review A* **95**, 012119, 1-7 (2017).
15. S. Altmeyer, Y.-H. Do, and Y.-C. Lai, "Dynamics of ferrofluidic flow in small aspect-ratio Taylor-Couette systems," *Scientific Reports* **7**, 40012, 1-19 (2017).
16. G.-L. Wang, H.-Y. Xu, L. Huang, and Y.-C. Lai, "Relativistic Zitterbewegung in non-Hermitian quantum photonic waveguide systems," *New Journal of Physics*, in press.
17. L. Ying and Y.-C. Lai, "Robustness of persistent currents in two-dimensional Dirac systems with disorders," *Physical Review B*, revised.

3 Accomplishments and New Findings

3.1 Conductance stability in chaotic and integrable quantum dots with random impurities

In the development of nano-scale quantum devices, an important issue is stability against random perturbations such as various types of impurities. While the impurities can be reduced to certain extent through improving and refining the underlying fabrication process, it is of interest to uncover alternative mechanisms to enhance the device stability. We demonstrated that classical chaos can be exploited to generate devices that are relatively more stable in the quantum regime than those with integrable dynamics.

Specifically, we studied quantum dot systems, an essential type of structures in nano-electronic devices. Such a system consists of a central scattering region, or a dot region, and a number of electronic waveguides (leads). Incoming electrons from one lead undergo scattering in the dot region and become outgoing in all leads. For quantum dots a fundamental phenomenon is universal conductance fluctuations with respect to variations in parameters such as the Fermi energy or the strength of an external magnetic field. For mesoscopic systems in the ballistic transport regime, at low temperatures the conductance fluctuations tend to be independent of the sample size and impurities and thus can serve as a probe of quantum chaos, a field aiming to uncover and understand the quantum manifestations of classical chaos. For over two decades quantum dot systems have been a paradigm to study quantum chaotic scattering, and there has been a large body of literature on the effects of distinct types of classical dynamics on conductance fluctuations. A basic result was that, for systems with integrable or mixed classical dynamics, the conductance curves typically contain a large number of Fano resonances, leading to sharp conductance fluctuations. But if the system has fully developed classical chaos, conductance fluctuations will be smooth. This result enables conductance fluctuations to be modulated through controlling the underlying classical dynamics.

The AFOSR support made it possible for us to address the problem of device stability with respect to random impurities. In particular, we considered ensembles of random impurities of systematically varying

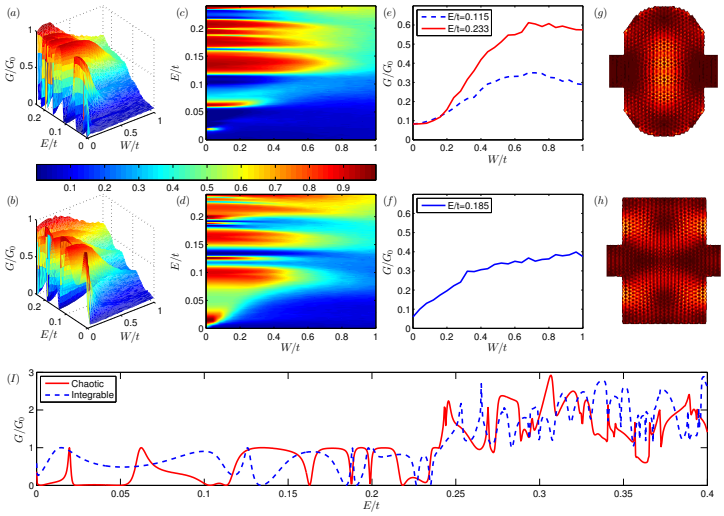

Figure 1: **Dependence of the average conductance on the Fermi energy and impurity strength**. (a,b) Three-dimensional plot of the conductance versus the Fermi energy and the impurity strength for classically chaotic and integrable dots, respectively. (c,d) The corresponding contour plots. (e) Two cases of resonance-like phenomenon for the chaotic geometry for $E/t \approx 0.115$ (red solid line), 0.233 (blue dashed line). (f) Conductance resonance for the integrable geometry for $E/t \approx 0.185$. (g,h) Examples of pointer states in absence of any random impurity for the chaotic and integrable cases, respectively. The device structural parameters are: lead width $w \approx 36.92\mathring{A}$, dot width $d \approx 78.7\mathring{A}$, and dot length $l \approx 151.94\mathring{A}$. (i) Conductances versus the Fermi energy of the chaotic (red solid line) and integrable (blue dashed line) devices without impurities. For both devices, the width of the first transmission mode is about $0.24t$. The results are in units of $G_0 = 2e^2/h$.

strength and investigate their effects on some *appropriately averaged value of the conductance*. For this purpose we analyzed quantum-dot systems of two semi-infinite leads, each supporting a *single* transverse mode, and focused on the average conductance over the corresponding single-mode Fermi-energy range. This energy range is classically small but quantum mechanically large, rendering applicable semiclassical treatment of the scattering dynamics. To contrast the role of classical dynamics, we chose two types of geometric domains for the dot region: stadium and rectangle, which generate classical chaotic and integrable dynamics, respectively. As the strength of the random impurities is increased from zero, the average conductance decreases due to localization of wavefunctions. However, we found that the integrable dot system exhibits a much faster decrease in the average conductance than that for the chaotic dot system, implying a stronger conductance stability for the latter. We developed a semiclassical theory to qualitatively explain this phenomenon, and also provide an understanding based on the random matrix theory through analyzing the local density of states in the dot region and the energy level statistics in the corresponding closed system. Our finding strongly advocates the use of chaotic geometry in quantum dot structures, which is consistent with previous results on smooth conductance fluctuations in classically chaotic systems. In general, classical chaos has the benefit of bringing in greater stability for quantum devices.

Some representative results are shown in Fig. 1. Details of this work can be found in

- G.-L. Wang, L. Ying, and Y.-C. Lai, "Conductance stability in chaotic and integrable quantum dots with random impurities," *Physical Review E* **92**, 022901, 1-10 (2015).

3.2 Conductance fluctuations in chaotic bilayer graphene quantum dots

Conductance fluctuations are a fundamental phenomenon in open quantum systems. An important result is universal conductance fluctuations (UCFs) in mesoscopic systems. The pioneering work of Lee and Stone

established theoretically that, for mesoscopic metal samples, when the inelastic diffusion length exceeds the sample dimensions, the conductance fluctuations are of the same order as the conductance quanta, which is independent of the sample size and of the degree of disorder at low temperatures, thereby exhibiting universal features. This result was consistent with both experimental studies and numerical simulations.

Since the discovery of graphene, the anomalous transport behavior of its charge carriers has attracted a great deal of attention. Conductance fluctuations in graphene systems have been studied experimentally and analyzed using the framework of UCFs. Rycerz *et al.* found theoretically that for strong disorder, the fluctuation behaviors agree with the Altshuler-Lee-Stone prediction. However, in the case of weak disorder, abnormally large conductance fluctuations (with magnitude several times larger than that in the strong disorder case) can occur, which can be attributed to the absence of backscattering due to the honeycomb lattice structure. Horsell *et al.* subsequently found that the variance of UCFs in both monolayer and bilayer graphene flakes is strongly affected by elastic scattering, particularly, intervalley scattering. Though the correlation of the fluctuations as a function of the Fermi energy is insensitive to the specific scattering mechanisms under common experimental conditions. For few-layer graphene flakes in contact with superconducting leads, conductance fluctuations can be enhanced if the applied voltage is smaller than the superconducting energy gap.

The seminal work of Jalabert, Baranger, and Stone suggested that conductance fluctuations in the ballistic regime can be a probe of quantum chaos, establishing for the first time a connection between quantum transport in solid-state devices and classical chaos. Subsequent works revealed that UCFs are intimately related to the study of quantum chaotic scattering. A result in nonrelativistic quantum chaotic scattering is that, for those with integrable or mixed (nonhyperbolic) classical dynamics, sharp conductance fluctuations can occur. This is because, in the corresponding classical phase space, there are Kolmogorov-Arnold-Moser (KAM) islands centered about stable periodic orbits, which quantum mechanically have little interaction between the corresponding bounded states and the electron waveguides (leads), leading to extremely sharp conductance fluctuations on energy scales of the same order of magnitude as the interaction energy. The abrupt conductance changes are in fact a kind of Fano resonance.

If the classical dynamics are chaotic, due to ergodicity of classical orbits, the states will have strong interactions with the leads regardless of their positions. As a result, there is little probability for localized states with long lifetime to form, giving rise to smooth conductance fluctuations in the energy scale determined by the interaction strength. The distinct types of classical dynamics thus have marked fingerprints in the quantum conductance fluctuation patterns, which can be exploited to modulate the conductance fluctuations in quantum dot devices by controlling the corresponding classical dynamics. In fact, a closed system exhibiting chaos in the classical limit is capable of generating scarred states in the quantum regime, which are concentrations of the electronic states about certain classical periodic orbits. However, when the system is open, the degree of localization of the originally scarred states is generally much weaker than that of the localized states in classically integrable or nonhyperbolic systems.

In relativistic quantum dots such as those made of monolayer graphene, our recent work revealed that systems with mixed classical dynamics exhibit sharper conductance fluctuations than those with chaotic classical dynamics, which is similar to nonrelativistic quantum systems. However, even when the classical dynamics are fully chaotic, monolayer graphene quantum dots still permit the existence of highly localized states, leading to Fano-like resonances with sharp conductance fluctuations. This implies that quasiparticles in a chaotic graphene confinement can make the classically unstable orbits somewhat more "stable" in relativistic quantum systems, implying that the interplay between chaos and relativistic quantum mechanics can lead to phenomena that are not present in nonrelativistic quantum systems.

A unique feature of monolayer graphene is that the quasiparticles are massless Dirac fermions. However, an open issue concerns about the interplay between *finite mass* and chaos in relativistic quantum transport. With the AFOSR support, we addressed the generality of persistently sharp conductance fluctuations in

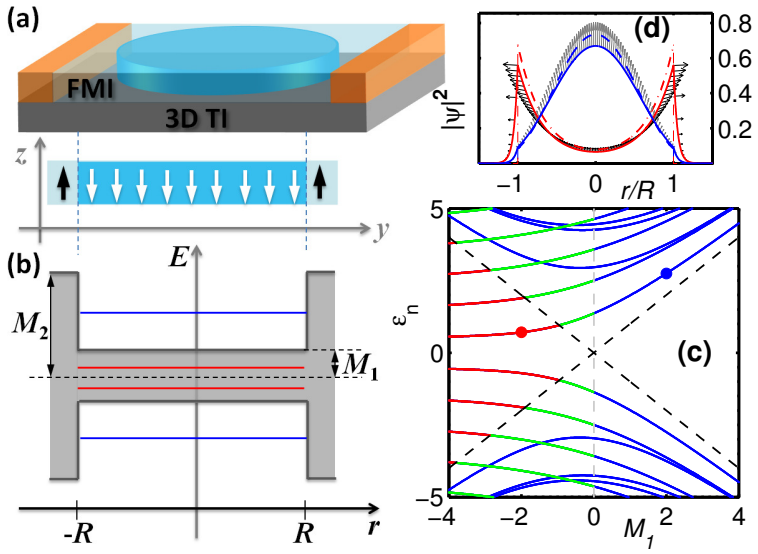

Figure 2: **Setup of a ferromagnetic insulator/topological insulator quantum dot system and some representative results**. (a) Schematic illustration of a quantum dot formed on the surface of a 3D topological insulator through a closed magnetic domain heterostructure of ferromagnetic insulators (e.g., EuS). (b) Schematic energy diagram of the dot system with mass confinement for zero applied field (R: dot radius; M_1 and M_2: dimensionless masses of the inner and outer regions, respectively). (c) Energy spectra of the dot structure in (b) as a function of M_1 for fixed $M_2 = 10$, where the blue curves denote the normal states and the black dash lines specify the insulating gap boundaries defined by M_1. The emergent edge states through a topological mechanism are divided into the under-gap and over-gap ones, denoted by the red and green curves, respectively. (d) Sectional view of the density distributions of the lowest positive energy states for $M_1 = \mp 2$ as indicated by the red and blue dots in (c). The red and blue curves are for the topological and normal states, respectively. Arrows denote the local spin orientation in the $S_x - S_z$ plane. The dashed/dot-dashed lines correspond to the case of hard-wall confinement, i.e., $M_2 \to +\infty$.

relativistic quantum chaotic systems. We used chaotic *bilayer* graphene quantum dots (BGQD) as a prototypical class of systems. The key feature of bilayer graphene is that the quasiparticles have a finite mass. We found that persistently sharp conductance fluctuations are still present in BGQDs, indicating that a finite mass is not capable of breaking down the localized states. Another finding was that, in bilayer graphene quantum dots, electrons tend to "hop" between the two layers along the classical ballistic trajectory in each layer. Thus, the local density of states (LDS) for one layer does not form an "orbit" *per se*: an "orbit" emerges only when the LDS for both layers are combined. Our results indicate that in both massless and massive chaotic relativistic quantum systems, Fano-like resonances and sharp conductance fluctuations are a common feature. While in nonrelativistic quantum systems, the resonances can be removed by making the system classically chaotic, the same cannot be expected in relativistic quantum systems. This may have implications in the development of relativistic quantum electronic devices.

Details of this work can be found in

- R. Bao, L. Huang, Y.-C. Lai, and C. Grebogi, "Conductance fluctuations in chaotic bilayer graphene quantum dots," *Physical Review E* **92**, 012918, 1-8 (2015).

3.3 Reverse Stark effect, anomalous optical transitions, and control of spin in topological insulator quantum dots

In systems exhibiting the conventional quantum-confined Stark effect (QCSE), e.g., a semiconducting quantum well, an external electrical field shifts the electronic states in the conduction band to lower energies

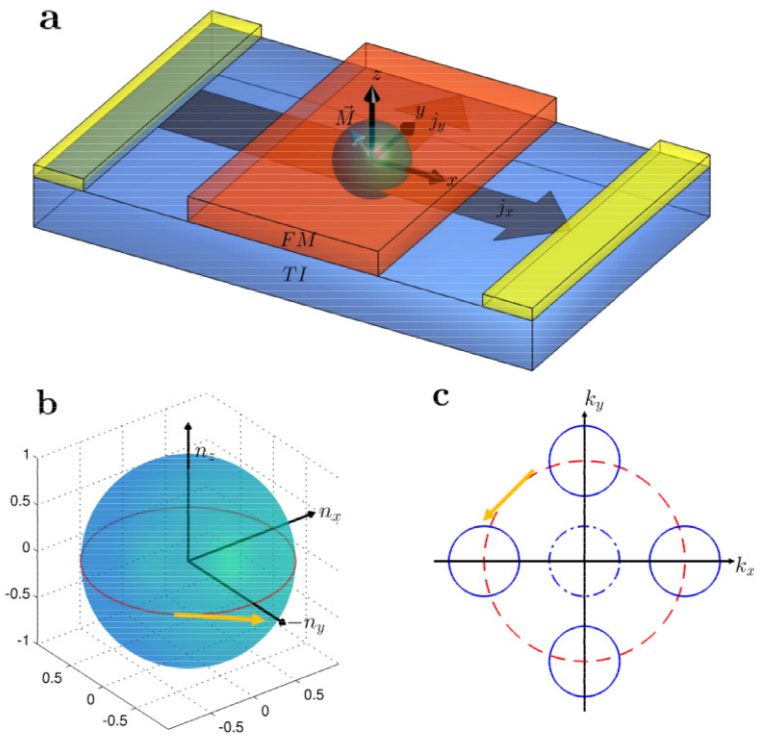

Figure 3: **Schematic illustration of the TI-FM coupled system and the basic interactions.** (**a**) A thin layer of insulating ferromagnet sits on a 3D TI. A voltage is applied along the x direction. The effective magnetization of the ferromagnet, $\boldsymbol{m}$, oscillates in time and is coupled to the spin-polarized currents j_x and j_y in the TI through the mechanism of exchange coupling. (**b**) A typical time evolution pattern of the normalized magnetization $\boldsymbol{n}$. (**c**) Change in the position of the Fermi surface in the wave vector space associated with the surface electrons of the TI, which corresponds to the adiabatic evolution of $\boldsymbol{n}$ in (**b**). The central dashed circle corresponds to the case where the ferromagnet is absent.

and the hole states in the valence band to higher energies. As a result, the energy differences between the electronic and hole states are narrowed, reducing the frequencies of the permitted photon absorption or emission. We discovered the intriguing phenomenon of reverse Stark effect: in topological Dirac materials an applied electrical field tends to *widen* the energy differences and consequently *increase* the light absorption or emission frequencies.

Uncovering, understanding, and exploiting exotic quantum phases are frontier problems in physics. Recent years have witnessed a great deal of effort in phase phenomena of certain topological origin. For example, 2D gapless topological phases were predicted and realized at the interface between bulk Bi_2Se_3 crystal and the vacuum, where a change in the Z_2 invariant from the former to the latter occurs. Inducing an energy gap by breaking the time-reversal symmetry in the vicinity of a magnetic material can lead to exotic phases of broken symmetry with dramatic physical consequences such as zero-field half-integer quantum Hall effect, topological magnetoelectric effect, and magnetic monopole. Topological effects in gapped Dirac materials are thus quite intriguing, where topologically protected chiral interfacial states carrying dissipationless currents can arise, which share the same mechanism as that for the Jackiw-Rebbi modes. More recently, it was demonstrated that tuning the topological behaviors through an electric field can lead to quantum spin Hall effect, bringing field-effect topological transistors closer to reality.

With the AFOSR support, we investigated the response of the topological states in a confined geometry, e.g., a quantum dot formed on the surface of a 3D topological insulator via a closed magnetic domain heterostructure, to an applied electric field. The system can be described by the Dirac equation subject to

proper mass confinement. With an inverted mass profile, a branch of quantized topological edge states can emerge. We found that, when an external electric field is applied, the under-gap topological states exhibit quite unusual alignments: the positive (negative) energy electronic states follow (align against) the direction of the field. As a result, a reverse QCSE occurs in that the frequencies of the permitted light absorption or emission *increase*. Remarkably, these states possess spin textures of ring-like in-plane polarization, which can be effectively controlled electrically or optically. We worked out an analysis based on solutions of the Dirac equation to explain these counterintuitive phenomena. The findings can have potential applications in Dirac material based optoelectronics and spintronics.

The setup of our ferromagnetic insulator/topological insulator quantum dot system and some representative results are shown in Fig. 2. Details of this work can be found in

- H.-Y. Xu and Y.-C. Lai, "Reverse Stark effect, anomalous optical transitions, and control of spin in topological insulator quantum dots," *Physical Review B* **92**, 195120, 1-6 (2015).

3.4 Nonlinear dynamics induced anomalous Hall effect in topological insulators

Hall effect is one of the most striking and widely investigated phenomena in contemporary physics. The classical Hall effect is simply due to the Lorentz force, while the quantum Hall effect can be attributed to the emergence of surface states due to the formation of Landau levels in a magnetic field, and the fractional quantum Hall effect results from many-body interactions. In certain materials, without any magnetic field, the spin-orbit interaction can lead to spin Hall effect, the physical base for topological insulators, an area of tremendous recent interest in condensed matter physics. We uncovered an alternative, dynamics based mechanism for the anomalous Hall effect. The underlying physics is spin-transfer torque.

Spin-transfer torque originates from the exchange coupling between the magnetization in a ferromagnet and a polarized spin current. When such a current flows close to the ferromagnet, a finite torque will be exerted on the magnetization of the ferromagnet, provided that the magnetization vector is not aligned with the direction of spin polarization. Semiclassically, the dynamical evolution of the magnetization can be described by the Landau-Lifshitz-Gilbert (LLG) equation. In spintronics applications, spin-transfer torque can be quite useful as it provides a way to manipulate or even switch, electronically, the magnetization in the ferromagnet, which can lead to reduced dimensions and efficient energy consumption as compared with conventional magnetic schemes. Previous studies on spin-transfer torque focused on heavy metals with strong spin-orbit coupling, which can generate significant spin-polarized current through the spin Hall effect or in materials with strong Rashba spin-orbit coupling effect at the interfaces. Another promising material is TIs that possess a bulk band gap but with metallic massless Dirac surface states. The strong Rashba-type SOC guarantees that the momentum of the surface electron is interlocked with its spin. When a TI is coated with a thin film of insulating ferromagnet, a host of novel magnetoelectric effects can arise. In this configuration, phenomena that have been predicted theoretically include the inverse spin-Galvanic effect, current-induced magnetization reversal, anomalous magnetoresistance of a two-dimensional ferromagnet/ferromagnet junction, and auto-oscillations of magnetization.

With the AFOSR support, we studied the dynamics of magnetization in the insulating ferromagnet as well as the spin-polarized current on the surface of TI. When the system is subject to a periodic electric driving signal with a *dc* offset applied to the the TI surface, rich nonlinear dynamical phenomena in magnetization can arise in the upper insulating ferromagnet via the induced spin-transfer torque, which include multistability, chaos, and phase synchronization. In certain range of the ratio of the *dc* and *ac* amplitudes, e.g., $[-1, 1]$, there are critical points at which the magnetization dynamics in the ferromagnet can change abruptly between two stable states (attractors), leading to adiabatic dynamical transport of the surface electrons in the 3D TI via the exchange coupling (i.e., the proximity effect). Our main finding was the emergence

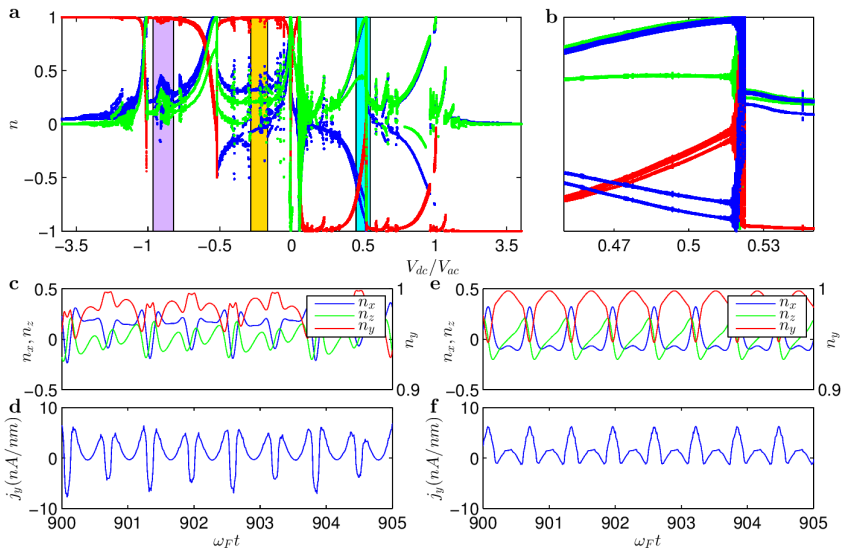

Figure 4: **Typical dynamical behaviors of the TI-FM coupled system.** (**a**) Bifurcation diagram of the magnetization with respect to ratio of applied dc and ac voltages. Blue, red and green dots correspond to n_x, n_y, and n_z, respectively. One chaotic regime is marked by a purple stripe and one phase-synchronization regime is marked by a yellow stripe. (**b**) Magnification of the transitional region in the bifurcation diagram in (**a**) (marked with cyan strip). (**c**) A representative time series of the magnetization from the purple chaotic regime. (**d**) Anomalous Hall current for a parameter value in (**b**). (**e**) A representative time series of the magnetization from the yellow phase synchronization regime, and (**f**) the corresponding anomalous Hall current. For better visualization, the x axis in (**a**) is rescaled.

on the surface of the TI of an unconventional Hall-like current resulting from the spin-transfer torque induced magnetization. This type of Hall effect is characterized by a multivalued functional relation between the transverse and longitudinal conductance. The nonlinear dynamical mechanism uncovered represents an alternative route to Hall effect. The dynamics-induced anomalous Hall effect can have potential applications in spintronics.

A schematic illustration of the TI-FM coupled system and the basic interactions is shown in Fig. 3. Some representative results nonlinear dynamical behaviors and anomalous Hall effect is shown in Fig. 4. Details of this work can be found in

- G.-L. Wang, H.-Y. Xu, and Y.-C. Lai, "Nonlinear dynamics induced anomalous Hall effect in topological insulators," *Scientific Reports* **6**, 19803, 1-9 (2016).

3.5 Enhancement of spin polarization by chaos in graphene

In a two-dimensional (2D) solid state system, when the potential in the direction perpendicular to the 2D plane is asymmetric, the atomic spin-orbit coupling can lead to a momentum-dependent splitting of the spin bands, a phenomenon known as the Rashba effect or the Rashba-Dresselhaus effect. This effect can be exploited for manipulating spin in various settings such as electrical spin injection, 2D superconducting devices, spin modulation through an electrical field, spin filtering, and spin field effect transistor. In two-dimensional Dirac materials of current interest such as graphene, topological insulators, and molybdenum disulfide (MoS_2), intrinsic or extrinsic spin-orbit interactions of various degrees can arise. The interaction typically leads to energy splitting and can result in fascinating phenomena such as the spin Hall effect, weak anti-localization, spin-flipping scattering and spin polarization. There are two types of spin-orbit coupling: intrinsic and external. In graphene, the intrinsic spin-orbit coupling is usually quite weak, but significant

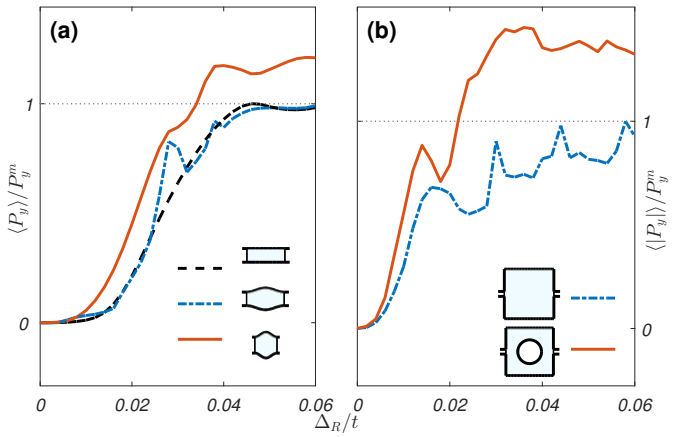

Figure 5: **Enhancement of spin polarization in graphene by classical chaos**. Average spin polarization versus Rashba interaction strength (a) for integrable (black dashed curve), nonhyperbolic (blue dashed-dotted curve), and hyperbolic (red solid curve) quantum dots, (b) for rectangular (blue dashed-dotted curve) and Sinai billiard (red solid curve) dot systems. The maximum spin polarization of integrable dots, P_y^m, is equal to 0.347 in (a) and 0.09 in (b). The side length of the rectangular billiard dot is $D = 118a$ and the lead width is $W = 6.5a$. The radius of the circular hard disk in the Sinai billiard system is $R = 0.258L$.

interaction (e.g., characterized by energy splitting on the order of 200meV) can be realized through the Rashba effect by depositing graphene on the surface of Ni(111) or Ir(111). Rashba spin-orbit interaction preserves the time-reversal symmetry but breaks the inversion symmetry in the direction perpendicular to the two-dimensional material plane, and has wide applications in spin transport devices. For example, for a two-terminal (source-drain) system with a Rashba field in the middle region, electrons of pure spin (say, spin up) are injected from the source and enter the central region. The Rashba coupling causes the electron spin to precess. When these electrons move into the drain terminal, some of them will have their spin flipped down. The flipping process leads to imperfect spin polarization. The degree of the spin polarization can then be modulated by the Rashba interaction strength.

In addition to the Rashba interaction strength, the geometric shape of the central interaction region can affect the electron scattering dynamics and, consequently, can have an effect on spin polarization. The central region where the Rashba coupling exists is the *scattering region*. Domains of different geometry can lead to characteristically distinct types of classical dynamics. For example, if the scattering region is rectangular, the underlying classical dynamics is integrable (or regular). However, a simple addition of two semicircular segments on two opposite sides of the rectangle leads to the stadium geometry, for which the classical dynamics is chaotic without any stable periodic orbits. If, a small circular region at the center of a square is converted into a classically forbidden region (e.g., through the application of a localized electrical potential), the domain becomes that of a Sinai billiard, for which the classical dynamics is fully chaotic with all periodic orbits being unstable. Our main finding was that chaos can enhance spin polarization, a beneficial property that can be exploited for spintronics applications.

We focused on a class of two-terminal graphene devices with Rashba interactions occurring in the central scattering region whose geometrical shape can be chosen to yield distinct types of dynamics in the classical limit. The shape of the scattering region is that of the cosine billiard with an upper and a lower hard boundaries at $y(x) = W + (M/2)[1 - \cos(2\pi x/L - \pi)]$ and $y = 0$, respectively, for $-L/2 \leq x \leq L/2$. To make the scattering region symmetrical, we chose the lower boundary to be

$$y(x) = \pm W + (M/2)[1 - \cos(2\pi x/L - \pi)]$$

for $-L/2 \leq x \leq L/2$, and the lead width is accordingly $2W$. The type of the classical dynamics in the billiard can be controlled by the parameter ratios W/L and M/L. For example, for $W/L = 0.18$ and $M/L = 0.11$, there are both stable and unstable periodic orbits, and the classical phase space is mixed (nonhyperbolic) with both chaotic regions and KAM islands. However, for $W/L = 0.36$ and $M/L = 0.22$, all periodic orbits are unstable and the classical dynamics is fully chaotic (hyperbolic). Given a billiard shape, we constructed the Hamiltonian incorporating Rashba interaction and use the Green's function method to calculate the conductance and spin polarization for systematically varied strength of the Rashba interaction. We found that, classical chaos can not only smooth the fluctuations of the spin polarization with the Fermi energy, but more importantly, can enhance the average spin polarization. We provided a heuristic argument based on semiclassical theory to understand the chaos-induced enhancement effect.

Representative results are illustrated in Fig. 5. A detailed account of this work can be found in

- L. Ying and Y.-C. Lai, " Enhancement of spin polarization by chaos in graphene quantum dot systems," *Physical Review B* **93**, 085408, 1-8 (2016).

3.6 A robust relativistic quantum two-level system

Two-level systems are fundamental not only to the development of quantum mechanics,, but also to quantum information processing and computing. Exploiting various physical systems to realize two-level operation has been an active area of research for a few decades. Among various types of two-level systems, superconducting and semiconductor-based systems are of particular interest. A basic requirement for an effective two-level system is that it provides two controllable states such as the direction of the circulating currents on a ring, the charge states in a double quantum dot, and the electron spin. The performance of the device is affected by the coupling of these states with the environment and by their robustness against material defects or various types of random interactions. For example, two-level operation in a double quantum dot system is sensitive to charge noise and electrostatic fluctuations induced by interface roughness or bulk defects. It is of general and continuous interest to articulate and develop two-level systems that are robust against random scattering and weak direct environmental coupling. In this regard, appealing features of Dirac materials include the emergence of topologically protected quantum states and long-range phase coherence, making them potential candidates for solid state two-level systems. Theoretical schemes have been proposed for graphene, topological insulators, and more recently the monolayer transitional metal dichalcogenides.

With the AFOSR support, we articulated a two-level system based on a class of relativistic quantum modes, the Dirac spinor-wave analog of the whispering galley modes (WGMs), as shown in Fig. 6. We considered the setting where a massless Dirac fermion is confined within a finite domain of ring topology, subject to a perpendicular magnetic flux at the center. The confinement can be generated from a mass potential, which can be experimentally realized using ferromagnetic insulators. A remarkable feature of the WGM type of spinor waves in the ring geometry is that they appear in pairs: one along the inner and another along the outer boundaries with oppositely circulating currents and spin polarizations, effectively forming a two-level relativistic quantum system. This Dirac system has peculiar spin textures as the coupling between the spin and current (momentum) constrains the spin directions into the plane transverse to the interface. The inner and outer states can be changed through tuning of the strength of the external magnetic field. The relativistic quantum two-level system is extremely robust against random scattering caused by boundary roughness and/or bulk electric disorders. Due to the breaking of the time-reversal symmetry (TRS) by the mass term, an insulator region is created. Based on the metal-insulator step junctions formed by spatially dependent mass potential in 2D Dirac fermion systems, we obtained an analytic argument to understand the origin of the robustness and the edge-dependent current/spin polarizations. A counter-intuitive feature is that, the inevitable boundary roughness and/or bulk defects are in fact desired, as they serve to introduce

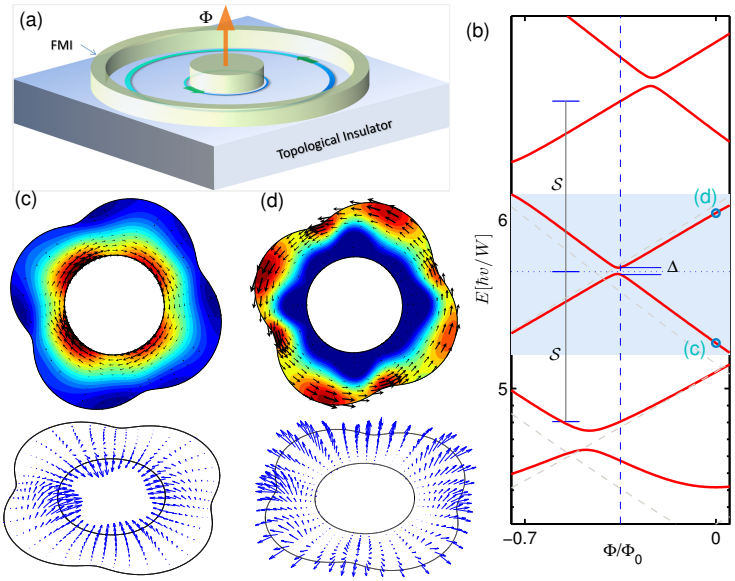

Figure 6: **Our proposed relativistic quantum two-level system**. (a) The system is patterned as a ring domain through the deposition of a ferromagnetic insulator (e.g., EuS) on the surface of the 3D TI, where a controllable mass potential is created through local exchange coupling (the proximity effect). (b) For $g = 0.5$, energy levels versus α, where the dashed lines show the circularly symmetric case for comparison. (c,d) The corresponding electronic densities and the associated charge current distribution (upper panels) and spin texture (lower panels) of the two adjacent Dirac WGMs indicated by the open circles in (b).

a finite coupling between the states, which is necessary for generating coherent oscillations through non-adiabatic sweeping of the external magnetic flux. We addressed the issue of decoherence and propose an experimental realization using 3D topological insulators (TIs). Our decoherence analysis based on a spin-boson model indicates that, for example, for a ring size of 100 nm, the quantum quality factor can be on the order of 10^4. Moreover, due to the TRS breaking confinement, our two-level system is less sensitive to electrostatic fluctuations than those based on conventional split-gate electrodes.

Details of this work can be found in

- H.-Y. Xu, L. Huang, and Y.-C. Lai, "A robust relativistic quantum two-level system with edge-dependent currents and spin polarization," *Europhysics Letters* **115**, 20005, 1-7 (2016).

3.7 Novel and unusual physics associated with scattering of pesudospin-1 particles

Solid state materials whose energy bands contain a Dirac cone structure have been an active area of research since the experimental realization of graphene. From the standpoint of quantum transport, the Dirac cone structure and the resulting pseudospin characteristic of the underlying quasiparticles can lead to unconventional physical properties/phenomena such as high carrier mobility, anti-localization, chiral tunneling, and negative refractive index, which are not usually seen in traditional semiconductor materials. Moreover, due to the underlying physics being effectively governed by the Dirac equation, relativistic quantum phenomena such as Klein tunneling, Zitterbewegung, and pair creations can potentially occur in solid state devices and be exploited for significantly improving or even revolutionizing conventional electronics. Uncovering/developing alternative materials with a Dirac cone structure has also been extremely active. In this regard, the discovery of topological insulators indicates that Dirac cones with a topological origin can be created, leading to the possibility of engineering materials to generate remarkable physical phenomena

such as zero-field half-integer quantum Hall effect, topological magneto-electric effect, and topologically protected wave transport.

A parallel line of research has focused on developing photonic materials with a Dirac cone structure, due to the natural analogy between electromagnetic and matter waves. For example, photonic graphene and photonic topological insulators have been realized, where novel phenomena of controlled light propagation have been demonstrated. Due to the much larger wavelength in optical materials as compared with the electronic wavelength, synthetic photonic devices with a Dirac cone structure can be fabricated at larger scales with greater tunabilities through modulations. The efforts have led to systems with additional features in the energy band together with the Dirac cones, opening possibilities for uncovering new and "exotic" physics with potential applications that cannot even be conceived at the present.

With the AFOSR support, we studied the basic transport physics in materials whose energy bands consist of a pair of Dirac cones and a topologically flat band, electronic or optical. For example, in a dielectric photonic crystal, Dirac cones can be induced through accidental degeneracy that occurs at the center of the Brillouin zone. This effectively makes the crystal a zero-refractive-index metamaterial at the Dirac point where the Dirac cones intersect with another flat band. Alternatively, configuring an array of evanescently coupled optical waveguides into a Lieb lattice can lead to a gapless spectrum consisting of a pair of common Dirac cones and a perfectly flat middle band at the corner of the Brillouin zone. As demonstrated more recently, loading cold atoms into an optical Lieb lattice provides another experimental realization of the gapless three-band spectrum at a smaller scale with greater dynamical controllability of the system parameters. With respect to creating materials whose energy bands consist of a pair of Dirac cones and a topologically flat band, there have also been theoretical proposals on Dice or $\mathcal{T}_3$ optical lattices and electronic materials such as transition-metal oxide $SrTiO_3$/$SrIrO_3$/$SrTiO_3$ trilayer heterostructures, 2D carbon or MoS_2 allotropes with a square symmetry, $SrCu_2(BO_3)_2$ and graphene-In_2Te_2 bilayer.

In spite of the diversity and the broad scales to realize the band structure that consists of two conical bands and a characteristic flat band intersecting at a single point in different physical systems, there is a unified underlying theoretical framework: generalized Dirac-Weyl equation for massless spin-1 particles. Such systems are pseudospin-1 Dirac cone systems. Comparing with the conventional Dirac cone systems with massless pseudospin/spin-$1/2$ quasiparticles (i.e., systems without a flat band), pseudospin-1 systems can exhibit quite unusual physics such as super-Klein tunneling for the two conical (linear dispersive) bands, diffraction-free wave propagation and novel conical diffraction, flat band rendering divergent dc conductivity with a tunable short-range disorder, unconventional Anderson localization, flat band ferromagnetism, and peculiar topological phases under external gauge fields or spin-orbit coupling. Especially, the topological phases arise due to the flat band that permits a number of degenerate localized states with a topological origin (i.e., "caging" of carriers). Most existing works, however, had focused on the physics induced by the additional flat band, and the scattering/transport dynamics in pseudospin-1 systems remains largely unknown (except the super-Klein tunneling behavior). Our main question was the following: what types of transport properties can arise form pseudospin-1 systems whose band structure is characterized by coexistence of a pair of Dirac cones and a flat band? To address this question in the simplest possible setting while retaining the essential physics, we studied ballistic wave scattering against a circularly symmetric potential barrier. It should be noted that for conventional Dirac cone systems with pseudospin or spin-$1/2$ quasiparticles, there has been extensive work on scattering with phenomena such as caustics, Mie scattering resonance, birefringent lens, cloaking, spin-orbit interaction induced isotropic transport and skew scattering, and electron whispering gallery modes. To our best knowledge, prior to our work there had been no corresponding studies for pseudospin-1 Dirac cone systems.

We investigated the scattering of pseudospin-1 particle from a circularly symmetric scalar potential barrier of height V_0 defined by $V(r) = V_0\Theta(R-r)$, where R is the scatterer radius and Θ denotes the Heaviside function. The band structure for the particle consists of a pair of Dirac cones and a flat band. Our main find-

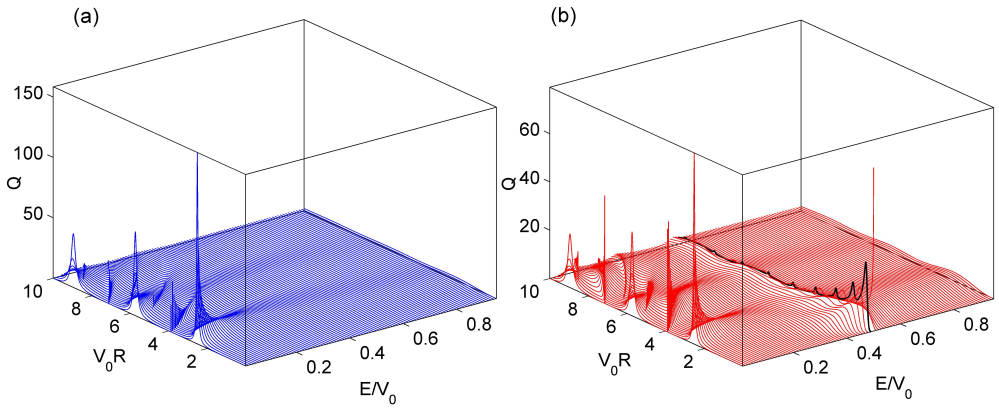

Figure 7: **Scattering efficient Q versus the scatterer strength V_0R and the relative incident energy** E/V_0 for (a) massless pseudospin-$1/2$ and (b) massless pseudospin-1 wave systems. The black curve is for $E/V_0 = 0.49$ with a highlighted visual effect.

ings were three: revival resonant scattering, super-Klein tunneling induced perfect caustics, and universal low-energy isotropic transport without broken symmetries for massless quasiparticles.

Revival resonant scattering. For small scatterer size, the effective three-component spinor wave exhibits revival resonant scattering as the incident wave energy is varied continuously, as shown in Fig. 7. Strikingly, the underlying revival resonant modes show a peculiar type of boundary trapping profile in their intensity distribution. While the profile resembles that of a whispering gallery mode, the underlying mechanism is quite different: these modes occur in the wave dominant regime through the formation of fusiform vortices around the boundary in the corresponding local current patterns, rather than being supported by the gallery type of orbits through total internal reflections.

Super-Klein tunneling induced perfect caustics. For larger scatterer size where the scattering dynamics are semiclassical, a perfect caustic phenomenon arises when the incident wave energy is about half of the barrier height, as a result of the super-Klein tunneling effect. A consequence is that the scatterer behaves as a lossless Veselago lens with effective negative refractive index resulting from the Dirac cone band structure. Compared with conventional Dirac cone systems for pseudospin-$1/2$ particles, the new caustics possess remarkable features such as significantly enhanced focusing, vanishing of the second and higher order caustics, and a well-defined static cusp. An illustration of the perfect caustics is presented in Fig. 8.

universal low-energy isotropic transport without broken symmetries for massless quasiparticles. In the far scattering field, an isotropic behavior arises at low energies, as shown in Fig. 9. Considering that there is no broken symmetry so the quasiparticles remain massless, the phenomenon is quite surprising as conventional wisdom would suggest that the scattering be anisotropic. By analyzing the characteristic ratio of the transport to the elastic time as a function of the scatterer size, we found that the phenomenon of scattering isotropy can be attributed to vanishing of the Berry phase for massless pseudospin-1 particles that results in constructive interference between the time-reversed backscattering paths. Because of the isotropic structure, the emergence of a Fano-type resonance structure in the function of the ratio versus the scatterer size can be exploited to realize effective switch of wave propagation from a forward dominant state to a backward dominant one, and vice versa. We developed an analytic theory with physical reasoning to

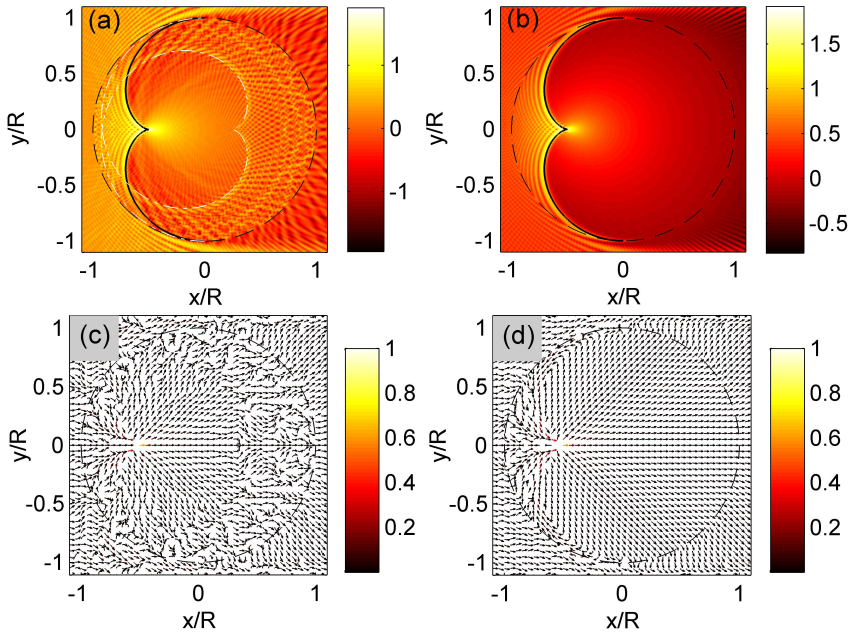

Figure 8: **Caustic behavior in the semiclassical regime and perfect caustics in pseudospin-1 Dirac cone systems**. The probability and local current density patterns, respectively, for (a,c) conventional pseudo-$1/2$ and (b,d) pseudospin-1 Dirac cone systems. The probability density patterns in (a) and (b) are plotted on a logarithmic scale. The corresponding local current density patterns in (c) and (d) are color-coded with magnitude normalized by its maximum. The parameters are $kR = 300$ and $E/V_0 = 1/2$.

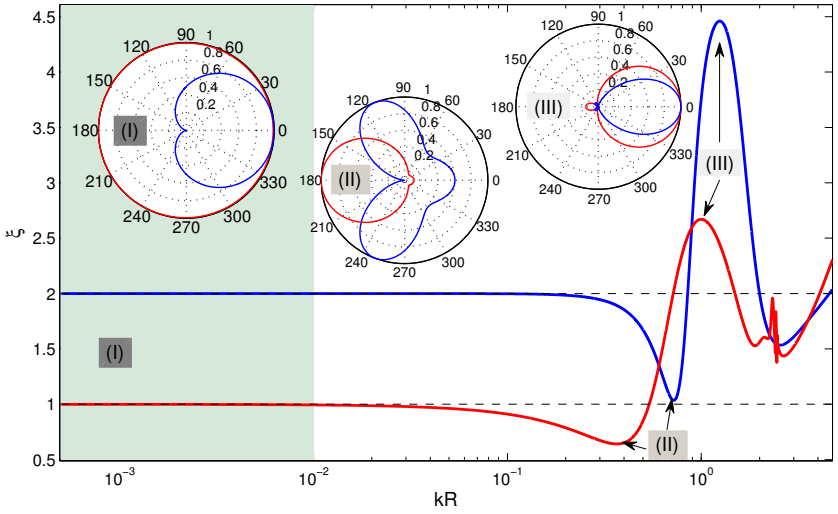

Figure 9: **Isotropic scattering of massless pseudospin-1 quasiparticle**. Ratio ξ as a function of kR for $V_0R = 5$: the red and blue lines are for the massless pseudospin-1 and pseudospin-$1/2$ cases, respectively.

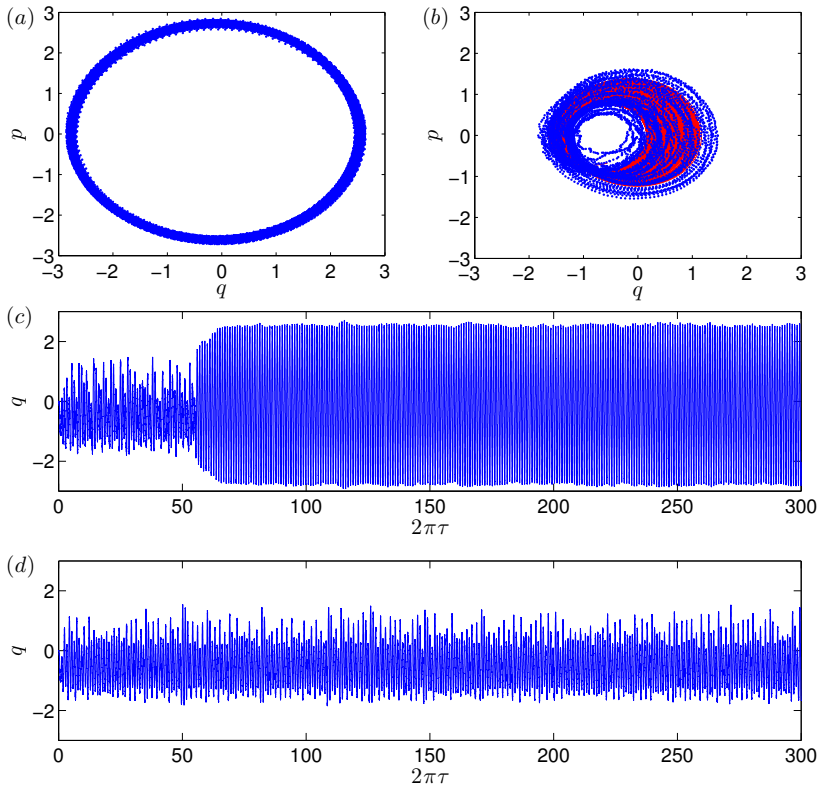

Figure 10: **A resolution of quantum-classical correspondence breakdown in an optomechanical system**. (a) An asymptotic quantum trajectory calculated from the QSD method, (b) the quantum trajectory in the transient phase, overlapped with the corresponding classical trajectory, (c) the corresponding time series. The asymptotic quantum trajectory is regular, in spite of the quantum fluctuations. However, the transient quantum trajectory is chaotic and coincides well with the classical trajectory (gray). (d) An example of a very long chaotic transient in the quantum regime.

understand the three novel phenomena, and articulated experimental verification schemes with photonic or electronic systems.

Details of this work can be found in

- H.-Y. Xu and Y.-C. Lai, "Revival resonant scattering, perfect caustics and isotropic transport of pseudospin-1 particles," *Physical Review B* **94**, 165405, 1-16 (2016).

3.8 Resolution of the paradox of breakdown of quantum-classical correspondence in optomechanics

The quantum-classical correspondence is a fundamental and fascinating problem in physics. For a specific physical process in a quantum system, if a large number of energy levels are involved (e.g., in the high energy regime), the evolution of the expected values of the observables will be governed by the classical Newtonian dynamics. This is the usual quantum-classical correspondence. Exceptions can occur when only a few lower energy levels are involved, e.g., at low temperatures, such that the quantum features of the ground state are manifested on a macroscopic scale, leading to fascinating phenomena such as Bose-Einstein condensation, superconductivity, and superfluids. Our discovery was that transient chaos serves as

a natural paradigm to explain the recently discovered phenomenon of the breakdown of quantum-classical correspondence in optomechanics.

A prototypical optomechanical system consists of an optical cavity with a fixed mirror and a nanoscale, mechanically movable cantilever. The basic physics is that the radiation pressure from the optical field changes the position of the movable mirror, which in return modulates the resonance frequency of the optical cavity, leading to a coupling between the optical and mechanical degrees of freedom. In addition to this prototypical setting, alternative configurations for realizing the optical-mechanical coupling exist, such as those based on the whispering-gallery modes, microtoroid and microsphere resonators. Optomechanics is thus not only fundamentally important, as it provides a setting to understand the physics of optical-mechanical interactions, but also practically significant with applications ranging from ultra-precision measurements, light-matter entanglement, mechanical memory, tunable optical coupler, classical state preparation through squeezing, optical transparency, and photon shuttling to creation of nonclassical light and cooling of microscopic or mesoscopic objects. The classical equations of motion of an optomechanical system are nonlinear, rendering possible chaotic behaviors.

A previous work demonstrated that, in the classical regime where the system exhibits chaos, in the corresponding quantum regime the motion becomes regular and no signatures of chaos appear to exist. This is the so-called *quantum-classical correspondence breakdown* in optomechanics. A conventional approach to studying the correspondence is to compare the quantum Wigner function distribution with the classical phase space distribution, both being average quantities. However, a recent work demonstrated an optimal state estimation for cavity optomechanical systems through Kalman filtering, which allows one to obtain the conditional system state in the presence of experimental noise. In addition, observation of quantum trajectories obeying quantum state diffusion through heterodyne detection in a coupled system between a superconducting qubit and an off-resonant cavity was reported, as well as other types of quantum trajectories. Thus, rather than focusing on the average properties of the system, we studied the individual quantum trajectories of the system as related to the continuous weak measurement to probe into the quantum-classical correspondence breakdown.

With the AFOSR support, we aimed to uncover, through systematic classical and quantum simulations, the dynamical and physical mechanisms responsible for the breakdown phenomenon. The standard treatment of an optomechanical system consists of quantizing the cavity optical field and the oscillations of the cantilever as two mutually interacting quantum boson fields while treating the driving laser field classically. Dissipation associated with the optical and mechanical fields can be incorporated into the quantum Langevin equations from the quantum input-output theory or by solving the quantum Master equation with the Lindblad operators. When chaos occurs in the classical limit, the system is typically in a high energy state with hundreds of photons and phonons, rendering infeasible direct simulation of the quantum Master equation. An effective framework is the method of quantum state diffusion (QSD), which generates quantum trajectories to approximate the time evolution as governed by the quantum Master equation. The QSD method has been instrumental to homodyne detection and the study of quantum-classical correspondence in dissipative quantum chaos. Here, using the QSD method, we calculated the dynamical trajectories of the system in the quantum regime. Our computations extending to the long time scales (which were not attempted in previous works) suggest that transient chaos associated with quantum trajectories is ubiquitous. (To our knowledge, in spite of reports of chaos, there had been no prior results of transient chaos in optomechanical systems.) In particular, before approaching a regular final state, the quantum system exhibits a behavior that is consistent with the classical chaotic behavior. Thus, in short and in long time scales, the time evolutions of the system in the quantum regime would appear to be chaotic and regular, respectively. This means that, in short time scales a quantum-classical correspondence does exist, but its breakdown occurs in the long time limit, as shown in Fig. 10. A striking finding was that, as the classical regime is approached, the average transient lifetime increases dramatically (faster than the Ehrenfest time - see Discussion). As the quantum system

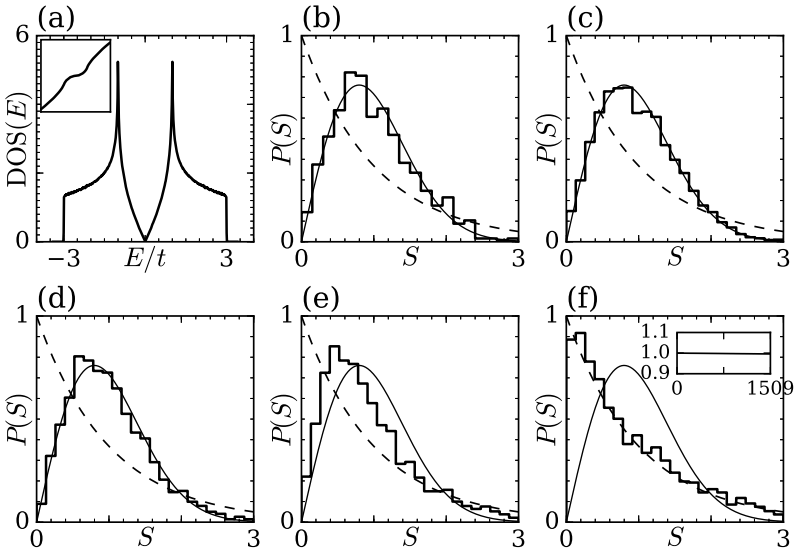

Figure 11: **Spectral properties of a graphene billiard with the shape of a** 15° **sector**. (a) The density of states. Inset: integrated density of states. (b-f) Nearest-neighbor spacing distributions in the energy ranges: (b) $E/t \in [0.02, 0.2]$, 837 levels; (c) $E/t \in [0.5, 0.6]$, 2575 levels; (d) $E/t \in [2.0, 2.1]$, 3804 levels; (e) $E/t \in [2.6, 2.7]$, 3321 levels; (f) $E/t \in [2.95, 3]$, 1509 levels. The histograms show the numerical results, the dashed and solid lines exhibit the Poisson and GOE distributions, respectively. Inset in panel (f): normalized ratio $(E - E_{edge})/E_{QB}$ for the first 1509 eigenenergies, where E_{QB} is the eigenenergy of the corresponding quantum billiards.

becomes "more classical," the quantum-classical correspondence holds significantly longer, providing a natural resolution for the breakdown phenomenon.

Details of this work can be found in

- G.-L. Wang, Y.-C. Lai, and C. Grebogi, "Transient chaos: breakdown of quantum-classical correspondence in optomechanics," *Scientific Reports* **6**, 35381, 1-13 (2016).

3.9 Unusual level statistics in graphene billiards

A fundamental result in quantum chaos, a field that studies the quantum signatures of classical chaos, is that distinct properties of the classical dynamics lead to characteristically different fluctuation properties in the energy spectra of the corresponding quantum system. In particular, for classically integrable systems, the energy levels behave like random numbers from a Poisson process, whereas the spectral properties of generic, classically chaotic systems coincide with those of the eigenvalues of random matrices from the Gaussian orthogonal ensemble (GOE), if time-reversal invariance is preserved. When time-reversal invariance is violated, the statistics is described by the Gaussian unitary ensembles (GUE). It should be noted that in nonrelativistic quantum chaotic systems, a magnetic field induces time-reversal symmetry breaking and changes the level statistics from GOE to GUE. Although the above correspondences may be violated for certain nongeneric cases, they are generally expected to hold for typical nonrelativistic quantum systems and even for relativistic quasiparticles in two-dimensional systems governed by the Dirac equation such as graphene flakes, also called graphene billiards.

Berry and Mondragon found in their seminal work that for relativistic neutrino billiards, i.e., massless spin-1/2 particles governed by the two-dimensional Dirac equation and confined to a bounded region, the spectral properties follow the Poisson statistics, if the shape of the confinement corresponds to a billiard

with classically integrable dynamics. Here, a billiard is a bounded two-dimensional domain inside which a pointlike particle moves freely and is reflected specularly at the walls. On the contrary, when the shape of the neutrino billiard corresponds to that of a classically chaotic billiard, the spectral properties agree with those of random matrices from the GUE, even in the absence of a magnetic field. This feature is attributed to the time-reversal invariance violation induced by the mass confinement.

Since the discovery of graphene, the fluctuation properties in the energy spectra of graphene billiards, i.e., finite-size graphene sheets formed by a single-layer of atoms arranged on a honeycomb lattice, have been investigated intensively. In view of the result of Berry and Mondragon on chaotic neutrino billiards, the spectral properties of chaotic graphene billiards were expected to follow GUE statistics. However, our extensive simulations using different chaotic graphene billiards clearly indicated GOE statistics. The physical mechanism for the GOE rather than GUE statistics has its origin in the hexagonal lattice structure of graphene which is composed of two independent triangular sublattices. As a consequence, the conduction and the valence band exhibit conically shaped valleys that touch each other at the six corners of the hexagonal first Brillouin zone, which, like the graphene lattice, is composed of two independent triangles, each corresponding to one of the two independent Dirac points. In each of the independent valleys the electron excitations are governed by a two-dimensional Dirac equation for massless spin-1/2 quasiparticles. The components of the associated pseudospin are related to the wave function amplitudes on, respectively, one of the triangular sublattices of the honeycomb lattice.

With the AFOSR support, we set out to understand the unusual level statistics in graphene billiards. The scattering at the boundaries of a finite-size graphene sheet leads to a mixing of the valleys. Accordingly, there the Dirac equations are coupled and the hexagonal lattice is described by a four-dimensional Dirac equation which preserves the time-reversal invariance. Naturally, it was speculated that a reduced degree of valley mixing might cause the level statistics to deviate from GOE toward GUE. In order to reduce mixing, we introduced a smoothly varying mass potential in the vicinity of the domain boundary in order to diminish the intervalley scattering. However, in general, the spectral statistics tended to GOE statistics irrespective of the residual scattering, which hence seems to be non-negligible. Consequently, GUE statistics may only be observed in graphene billiards with zigzag edges formed by atoms from the same sublattice like in an equilateral triangle. In this case, introducing a smoothly varying disorder potential will induce a transition from Poisson statistics to GOE statistics, if all three sides are formed by zigzag edges, and to GUE statistics if the sheet is terminated by armchair edges. We showed that, if a zigzag triangular nanoflake is deformed so that it does not possess any geometric symmetry, a strain-induced gauge field can effectively break the time-reversal symmetry, leading to GUE statistics. Furthermore, we studied the effects of random disorder and edge roughness with the result that increasing disorder or edge roughness is accompanied by a transition from Poisson to GOE statistics.

Current understanding of the energy level statistics of graphene billiards can be summarized as follows. Without magnetic field, if the shape of the bounded domain leads to a classically integrable dynamics, the spectral fluctuations coincide with that of Poisson random numbers. If the shape of the confinement coincides with that of a billiard with classically chaotic dynamics, the statistics is described by the GOE. We found counterintuitive features of the spectral statistics: finite-size graphene sheets with the shapes of certain classes of classically integrable billiards generically exhibit GOE statistics, as exemplified in Fig. 11. This finding was established through a combination of numerical simulations and physical reasoning.

Details of this work can be found in

- P. Yu, Z.-Y. Li, H.-Y. Xu, L. Huang, B. Dietz, C. Grebogi, and Y.-C. Lai, "Gaussian orthogonal ensemble statistics in graphene billiards with the shape of classically integrable billiards," *Physical Review E* **94**, 062214, 1-12 (2016).

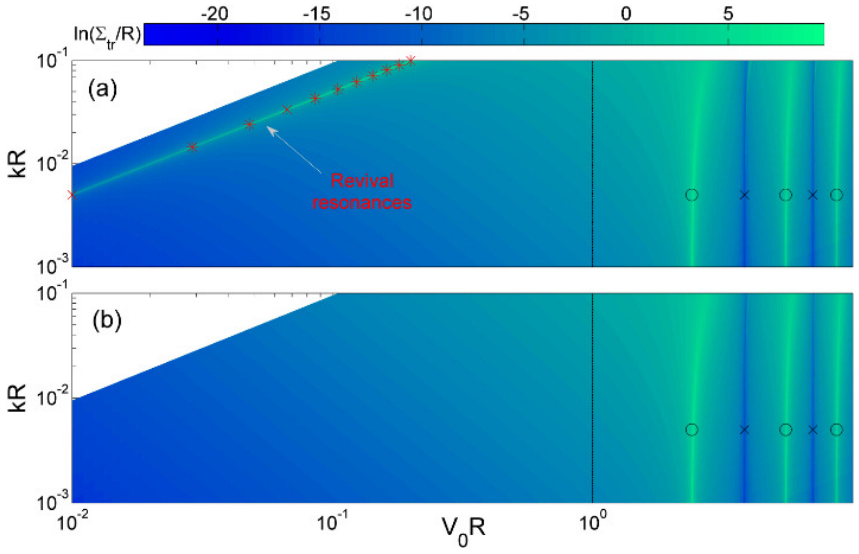

Figure 12: **Persistent revival resonances of pseudospin-1 particles from a weak circular scatterer at low energies**. (a) Contour map of transport cross section in unit of R (on a logarithmic scale) versus the scatterer strength $\rho = V_0 R$ and size $x = kR$ for relativistic quantum scattering of 2D massless pseudospin-1 particles. Revival resonances occur, leading to superscattering). (b) Similar plot for pseudospin-1/2 particles for comparison, where no resonances occur, implying total absence of superscattering. The scatterer is modeled as a circular step like potential $V(r) = V_0\Theta(R-r)$, representing a finite size scalar impurity or an engineered scalar-type of scatterers. The markers correspond to the theoretical prediction, where the black circles ($\circ$) and crosses ($\times$) are from $\rho \approx \rho_{0,m}, \rho_{1,n}$ (for $x \ll 1$), and the red stars ($*$) follow the revival resonant condition given by $\rho = 2x$ for $\rho \ll 1$.

3.10 Superscattering of pseudospin-1 wave in a photonic lattice system

In wave scattering, a conventional and well accepted notion is that weak scatterers lead to weak scattering. This can be understood by resorting to the Born approximation. Consider a simple 2D setting where particles are scattered from a circular potential of height V_0 and radius R. In the low energy (long wavelength) regime $kR < 1$ (with k being the wavevector), the Born approximation holds for weak potential: $(m/\hbar^2)|V_0|R^2 \ll 1$. Likewise, in the high energy (short wavelength) regime characterized by $kR > 1$, the Born approximation still holds in the weak scattering regime: $(m/\hbar^2)|V_0|R^2 \ll (kR)^2$. In general, whether scattering is weak or strong can be quantified by the scattering cross section. For scalar waves governed by the Schrödinger equation, in the Born regime the scattering cross section can be expressed as polynomial functions of the effective potential strength and size. For spinor waves described by the Dirac equation (e.g., graphene systems), the 2D transport cross section is given by $\Sigma_{tr}/R \simeq (\pi^2/4)(V_0R)^2(kR)$ (under $\hbar v_F = 1$). In light scattering from spherically dielectric, "optically soft" scatterers with relative refractive index n near unity, i.e., $kR|n-1| \ll 1$, the Born approximation manifests itself as an exact analog of the Rayleigh-Gans approximation, which predicts that the scattering cross section behaves as $\Sigma/(\pi R^2) \sim |n-1|^2(kR)^4$ in the small scatterer size limit $kR \ll 1$. In wave scattering, the conventional understanding is then that a weak scatterer leads to a small cross section and, consequently, to weak scattering, and this holds regardless of nature of the scattering particle/wave, i.e., vector, scalar or spinor.

With the AFOSR support, we uncovered a counterintuitive phenomenon that defies the conventional wisdom that a weak scatterer always results in weak scattering. The phenomenon occurs in scattering of higher spinor waves, such as pseudospin-1 particles that can arise in experimental synthetic photonic systems whose energy band structure consists of a pair of Dirac cones and a flat band through the conical intersection point. Theoretically, pseudospin-1 waves are effectively described by the generalized Dirac-

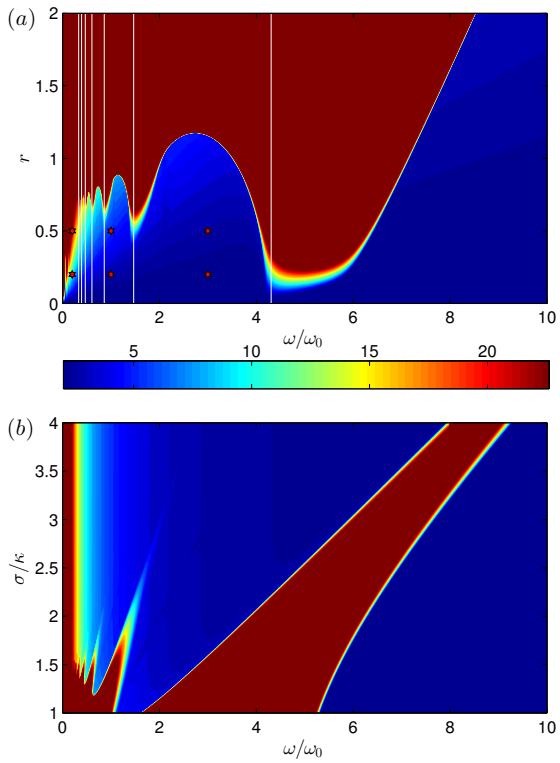

Figure 13: **Phase diagrams of relativistic quantum photonic superlattice system**. The dark red region indicates the pseudo-$\mathcal{PT}$ breaking phase, and the other region corresponds to the pseudo-$\mathcal{PT}$ phase. (a,b) Phase diagrams in the $r-\omega$ and $\sigma_r-\omega$ parameter plane, respectively. The color is coded in terms of the logarithm of the maximum intensity in the specific parameter region. The white lines in (a) denote the positions of the valleys in the oscillatory variations of the boundary. For each phase diagram, the computational grid in the corresponding parameter plane has the size 512×512. The parameters are $\sigma_r/\kappa=2.1$ (a) and $\sigma_i/\kappa=0.5$ (b).

Weyl equation $H_0\Psi=\boldsymbol{S}\cdot\boldsymbol{k}\Psi=E\Psi$ with $\Psi=[\Psi_1,\Psi_2,\Psi_3]^T$, $\boldsymbol{k}=(k_x,k_y)$ and $\boldsymbol{S}=(S_x,S_y)$ being the vector of 3×3 matrices for spin-1 particles. Investigating the general scattering of pseudospin-1 wave, we found the surprising and counterintuitive phenomenon that extraordinarily strong scattering, or superscattering, can emerge from arbitrarily weak scatterers at sufficiently low energies (i.e., in the deep subwavelength regime), as exemplified in Fig. 12. Accompanying this phenomenon is a novel type of resonances that can persist at low energies for weak scatterers. We provided an analytic understanding of the resonance and derive formulas for the resulting cross section, with excellent agreement with results from direct numerical simulations. We also proposed experimental verification schemes using photonic systems.

Details of this work can be found in

- H.-Y. Xu and Y.-C. Lai, "Superscattering of pseudospin-1 wave in photonic lattice," *Physical Review A* **95**, 012119, 1-7 (2017).

3.11 Relativistic Zitterbewegung in non-Hermitian photonic systems

There has been a great deal of recent interest in investigating the role of parity-time reversal ($\mathcal{PT}$) symmetry in wave propagation at different scales with the discoveries of phenomena such as non-reciprocal beam propagation, and uni-directionally transparent invisibility. The phenomenon of topologically protected states was originally discovered in condensed matter physics associated with electronic transport, but recently it has been demonstrated in optics, due naturally to the correspondence between matter and optical waves. For example, topological photonics/acoustics were demonstrated by exploiting the analogy between electronic and synthetic photonic crystals, where tunable and topologically protected excitations were observed. There were also efforts in exploring new wave features in artificial photonic crystals with/without the $\mathcal{PT}$-symmetry. All these have led to the emergence of a forefront area of research in optics: light

propagation in non-Hermitian $\mathcal{PT}$-symmetric media with balanced loss and gain profiles. The new field offers the possibility to engineer light propagation, potentially revolutionizing optics with unconventional applications.

In conventional quantum mechanics, the observable operators are required to be Hermitian to ensure real eigenvalues. This requirement is the result of one of the fundamental postulates in quantum mechanics: the physically observable or measurable quantities are the eigenvalues of the corresponding operators. However, the seminal works of Bender *et al.* demonstrated that non-Hermitian Hamiltonians are also capable of generating a purely real eigenvalue spectrum and therefore are physically meaningful, if the underlying system possesses a $\mathcal{PT}$ symmetry. This opened a new research field called non-Hermitian $\mathcal{PT}$ symmetric quantum mechanics. In fact, in physical systems, non-Hermitian Hamiltonians exist in contexts such as electronic transport (in open Hamiltonian systems) and gain/loss materials in optics. Especially, in optics, materials with a complex index of refraction can effectively be a non-Hermitian $\mathcal{PT}$ symmetric system. However, in such a case, the $\mathcal{PT}$ symmetry constrictions require that the real and the imaginary parts of the refractive index be an even and odd function in space, respectively, which may be challenging to be fabricated for experimental study. An alternative configuration that does not require even/odd spatial functions is the pseudo-$\mathcal{PT}$ symmetric system with periodic modulations. While such a system does not conserve the energy at any given instant of time because of gain/loss, the energy does not diverge within any practically long time.

With the AFOSR support, we addressed the outstanding problem of how *relativistic* quantum effects manifest themselves in non-Hermitian photonic systems with full or pseudo $\mathcal{PT}$ symmetry. This was motivated by the tremendous development of 2D Dirac materials in the past decade. It is thus of interest to investigate experimentally more realizable optical systems hosting relativistic excitations and to study the manifestations of the fundamental phenomena such as the Klein tunneling, *Zitterbewegung* (ZB), and pseudo spin to exploit their topological origin. In this regard, including gain/loss in synthetic optical systems can generate non-Hermitian relativistic $\mathcal{PT}$-symmetric excitations through engineering the gain and loss in a balanced manner. For example, arranging $\mathcal{PT}$-symmetric couplers periodically provides a unique platform to realize the analogy of the non-Hermitian relativistic quantum systems in optics.

With the AFOSR support, we focused on a fundamental phenomenon in relativistic quantum mechanics - ZB oscillations. While the optical analog of the relativistic ZB effect in Hermitian quantum systems was previously observed, we investigated the manifestations of ZB in non-Hermitian photonic systems. In particular, we considered a binary waveguide array with periodically modulated imaginary refraction index in the guiding direction. This kind of time-periodic gain and loss photonic system is widely used in many theoretical and experimental works. The optical waveguide array system, due to its controllable degrees of freedom, has been a paradigm to study a host of fundamental physical phenomena such as the neutrino oscillations, Bloch oscillation, Zener tunneling, and Klein tunneling. We configured the system to have a pseudo-$\mathcal{PT}$ symmetry, so that it exhibits quasi-stationary light propagation with slowly varying time-averaged total intensity. By calculating a detailed phase diagram (exemplified in Fig. 13) in an experimentally meaningful parameter space, we uncovered a number of phenomena in the system. In particular, we found that, in certain parameter regime, the wave amplitude tends to diverge. A remarkable phenomenon is that there are parameter regimes in which the dependence of ZB oscillations on the modulation frequency is non-monotonic, where the system exhibits a striking, periodically suppressed ZB effect with revival or intermittent ZB oscillations for low frequencies and a Hermitian-like ZB effect in the high frequency regime, as shown in Fig. 14. In the intermediate frequency regime, a surprising spatial energy localization behavior emerges. By solving the corresponding time-dependent Dirac equation, we obtained analytic results that provide explanations for the numerically observed, ZB manifested phenomena. The findings have implications. For example, the wave divergence phenomenon may be exploited for applications in optical amplifier and lasing. Intermittent BZ oscillations can potentially lead to a new mechanism to manipulate/control light

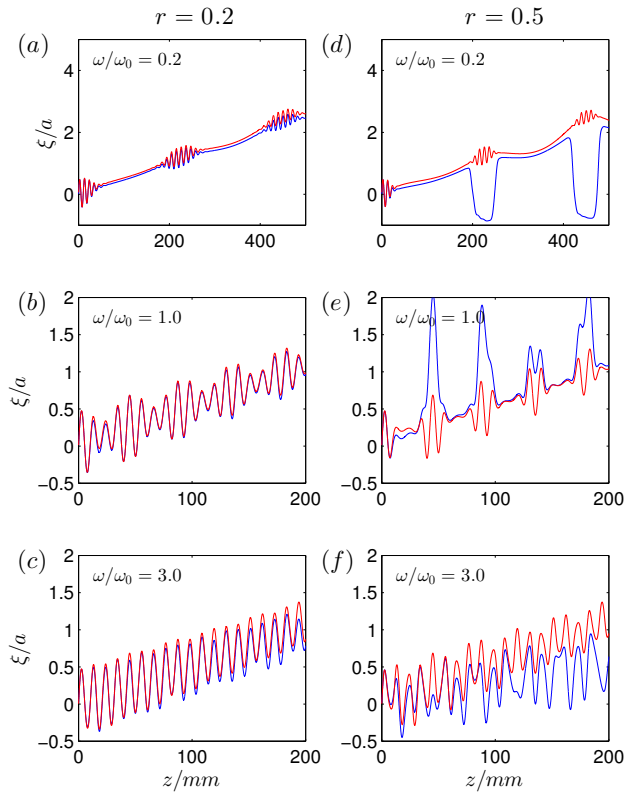

Figure 14: **Relativistic *Zitterbewegung* in non-Hermitian photonic superlattice systems**. The six panels correspond to all possible combinations of $r = 0.2, 0.5$ and $\omega/\omega_0 = 0.2, 1.0, 3.0$, as marked by the red stars in Fig. 13(a). (a-c) Mean/expectation values of the position of the wave packet for $r = 0.2$ and $\omega/\omega_0 = 0.2, 1.0, 3.0$, respectively. (d-f) Similar plots but for $r = 0.5$. The blue and red curves correspond to the beam center of mass of the wave packet from the simulation results and the mean expectation value of the position operator from the analytic results, respectively.

propagation.

Experimentally, conventional non-Hermitian PT-symmetry systems require that the real part of the effective potential to be an exactly even while the imaginary part be an exactly odd function in space. Our system design *relaxes* these requirements and significantly expands the configuration range of the non-Hermitian systems through introducing spatial modulation. The width of ZB trembling is on the order of micrometer and the length of the waveguides is millimeters. Concretely, our system can be realized in a waveguide array configuration where the gain effect can be realized, for example, through doping of dye molecules such as Rhodamine B (emission at 627 nm, excitation at 554 nm - green laser). Loss can be introduced using metals evaporated into the waveguides during the fabrication process.

Details of this work can be found in

- G.-L. Wang, H.-Y. Xu, L. Huang, and Y.-C. Lai, "Relativistic Zitterbewegung in non-Hermitian quantum photonic waveguide systems," *New Journal of Physics*, in press.

3.12 Robustness of persistent currents in two-dimensional Dirac systems with disorders

Persistent or permanent currents, i.e., currents requiring no external voltage with zero resistance, were traditionally thought to occur only in superconductors. However, about three decades ago, it was theoretically predicted that such dissipationless currents can emerge in normal metallic or semiconductor ring systems subject to a central Aharonov-Bohm (AB) magnetic flux. In particular, if the ring size is smaller than the quantum phase coherent length, the electron motion in the entire domain will become ballistic, effectively eliminating scattering. If the ring size is larger than the phase coherent length, the electron's behavior will

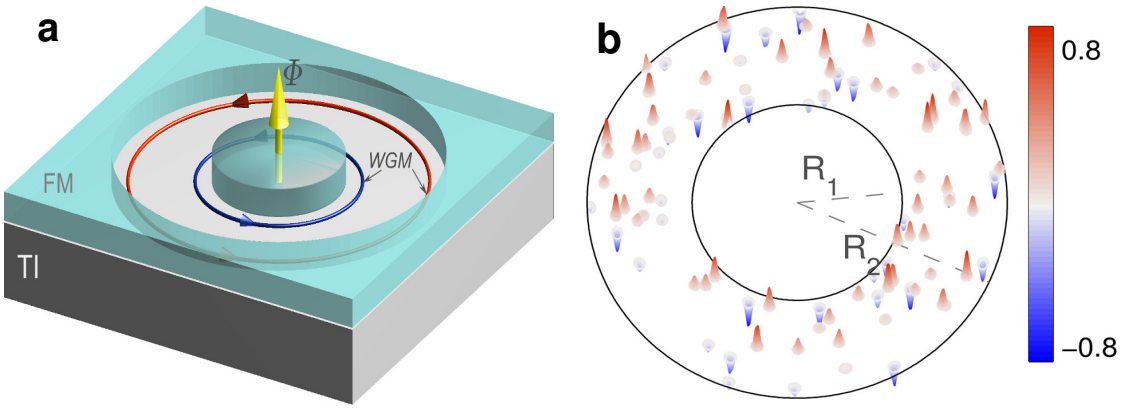

Figure 15: **Schematic illustration of a ring domain with an AB magnetic flux through the center**. (a) The light blue color denotes the regions of infinite mass. Red and blue loops illustrate the eigenstates near the outer and inner boundaries, respectively. (b) Schematic illustration of random disorders uniformly distributed in the ring region, with their strength denoted with different colors. Experimentally a Dirac ring can be generated by placing a ferromagnetic insulator of proper shape on the surface of a topological insulator.

be diffusive with a current proportional to $1/\tau_D$, where τ_D is the diffusion time around the ring. While the environmental temperature needs to be sufficiently low to reduce inelastic scattering from phonon-electron and/or electron-electron interactions for the currents to be observed, the metallic material itself remains "normal" (i.e., not superconducting). The remarkable phenomenon of persistent currents was subsequently observed experimentally in a large variety of settings, all being nonrelativistic quantum systems.

Persistent currents in nonrelativistic quantum systems are vulnerable to material impurities, which fundamentally restricts the phenomenon to systems at or below the mesoscopic scale. Indeed, in real materials disorders are inevitable, which can dramatically reduce the phase coherent length due to enhanced random scattering. In general, random disorders can remove the energy degeneracies and induce level repulsion, opening energy gaps and destroying the conducting state. As a result, disorders in metallic or semiconductor systems, 1D or 2D, tend to diminish the persistent currents. As the strength of the disorder is increased, the currents decay exponentially to zero.

There were studies of persistent currents, e.g., in graphene and other Dirac materials. The effects of boundary deformation on the persistent currents were recently investigated, where it was found that, even when the deformation is so severe that the corresponding classical dynamics in the 2D domain becomes fully chaotic, persistent currents can sustain. The physical origin of the so-called superpersistent currents can be attributed to the emergence and robustness of a type of quantum states near the boundaries of the domain, which carry a large angular momentum and correspond essentially to the whispering gallery modes (WGMs) that arise commonly in optical systems and can occur in nonrelativistic quantum electronic systems as well. The Dirac WGMs are insensitive to boundary deformations, which may be intuitively understood as a consequence of the zero flux boundary condition required for nontrivial, physically meaningful solutions of the Dirac equation. In spite of these efforts, the effects of bulk disorders on persistent currents in 2D Dirac systems remains to be an open issue. In particular, since there are random scattering sources inside the domain with a finite probability of occurrence even near the boundary, it is not intuitively clear whether the Dirac WGMs and hence persistent currents can still exist when there are random impurities in the ring domain.

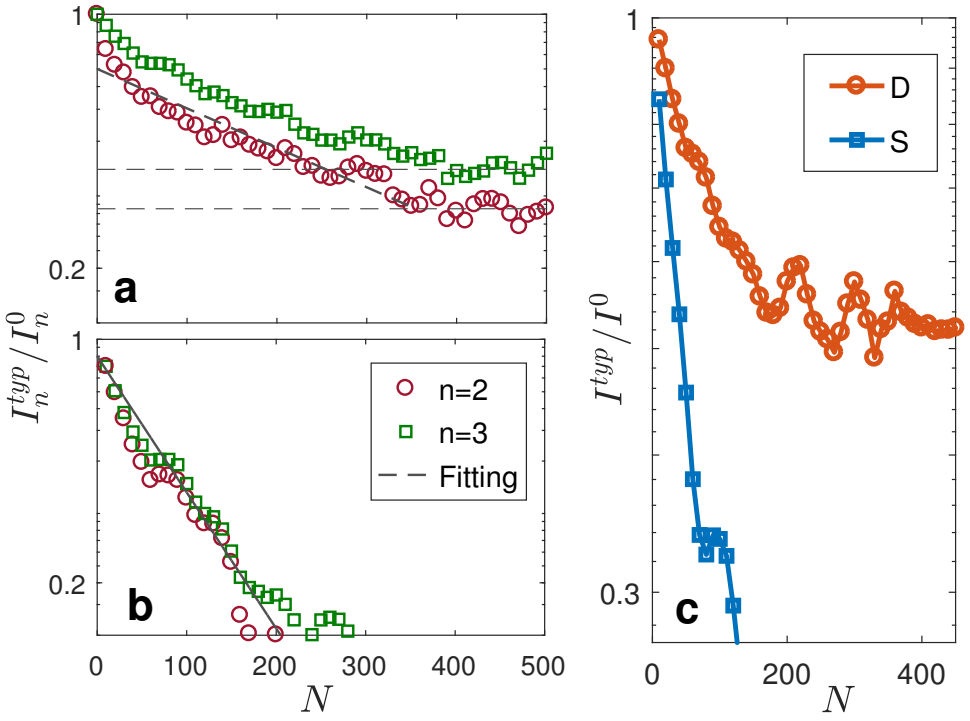

Figure 16: **Robustness of persistent currents in Dirac ring against random disorders**. Typical single-level persistent currents versus the number of the disorders for (a) Dirac and (b) Schrödinger rings, for fixed disorder strength $u_m^{(D,S)} = 300\Delta E_{10}^{(D,S)}$. The mean radius of a single impurity is $\delta r = (1-\xi)/20$. (c) The average persistent current versus the number of the disorders for $n_{max} = 5$, where other parameters are the same as in (a,b) for the Dirac (denoted as "*D*" and illustrated as circles) and Schrödinger (denoted as "*S*" and displayed as squares) rings. The range of the number of disorders, $N \in [0, 500]$, corresponds to the range of the ratio between the disorder and ring areas $S_{dis}/S_{ring} \in [0, 0.43]$.

In our study, investigated the effects of random disorders on persistent currents in 2D relativistic quantum systems. To be concrete, we considered a Dirac ring domain with a vertical magnetic flux through the center. To completely constrain a Dirac fermion within the domain, we imposed the infinite mass boundary condition originally introduced by Berry into the study of chaotic neutrino billiard, which is experimentally realizable through a proper arrangement of ferromagnetic insulation. We assumed uncorrelated disorders throughout the domain, which can be simulated using localized, random electric potential uniformly distributed in the domain, as illustrated in Fig. 15. In an experiment, for a given material, neither the strength nor the density of the disorders can be readily adjusted. However, the sample size can be controlled. Classically, under a vertical magnetic field, the electrons move along circular trajectories in the domain. In experiments, for a larger ring sample with constant disorder density, an electron encounters more disorders/scattering events in one complete rotation. For computational convenience, we fixed the outer radius of the ring domain to be unity. In this case, varying the disorder density is equivalent to changing the size of ring domain, where a higher density corresponds to a larger domain. Following this heuristic consideration, we fixed the disorder strength as well as the domain size but systematically vary the density of the disorders. For convenience, in our computations we set the total number of disorders in the whole domain as a control parameter, and solve the Dirac equation to obtain the magnitudes of the persistent currents as a function of the number of disorders. For comparison with the nonrelativistic quantum counterpart, we solved the Schrödinger equation under the same setting.

Our main results were the following. For the Dirac ring system, as the number of the disorders is systematically increased, the average current decreases slowly initially and then plateaus at a finite nonzero value,

indicating that the persistent currents are robust, as exemplified in Fig. 16. We demonstrated that WGMs are the physical mechanism responsible for the robust currents. In contrast, in the nonrelativistic quantum ring system, the WGMs are sensitive and fragile to the disorders, leading to a rapid and exponential decay of the currents to zero. We developed a physical theory based on a quasi one-dimensional approximation to understand the strikingly contrasting behaviors of the currents in the Dirac and Schrödinger rings. An important implication of our finding is that persistent currents in the Dirac rings can occur in realistic systems of large size.

Details of this work can be found in

- L. Ying and Y.-C. Lai, "Robustness of persistent currents in two-dimensional Dirac systems with disorders," *Physical Review B*, revised.

4 Personnel Supported and Theses Supervised by PI

4.1 Personnel Supported

The following people received salaries from the AFOSR Project during various time periods.

- **Faculty**: Ying-Cheng Lai (PI), Chair Professor of Electrical Engineering, Professor of Physics.
- **PhD Students**:
  1. Lei Ying (graduated in August 2016)
  2. Hongya Xu (passed Ph.D. defense in December 2016)
  3. Guanglei Wang (to defend Ph.D. thesis in Spring 2017)
  4. Chengzhen Wang (ongoing).

4.2 PhD graduates who participated in research in the project area

1. Lei Ying, Electrical Engineering, ASU, August 2016. Dissertation: *Quantum nonlinear dynamics in graphene, optomechanical, and semiconductor superlattice systems*.
2. Hong-Ya Xu, Electrical Engineering, ASU, December 2016. Dissertation: *Electrical, spin, and valley transport in two-dimensional Dirac systems*.

5 Interactions/Transitions

5.1 Collaboration with DoD scientists

- Dr. Danhong Huang from Air Force Research Laboratory in Albuquerque, on nonlinear dynamics in semiconductor superlattice systems and quantum valley Hall effect in Dirac material systems.

5.2 Invited talks on topics derived from the project

During the project period, PI gave the following invited plenary talks and seminars on various topics derived from AFOSR sponsored research.

1. "Relativistic quantum chaos," Opening plenary talk, Third National Statistical Physics and Complex Systems Conference, Lanzhou, China; July 22, 2015.
2. "Nonlinear dynamics and chaos in micro/nano-scale systems and applications," Invited talk, Session of Engineered Micro Systems/Devices, IMAPS 12th International Conference and Exhibition on Device Packaging, Fountain Hills, Arizona; March 16, 2016.
3. "Relativistic Quantum Chaos," Plenary talk, International Conference on Perspective in Nonlinear Dynamics 2016, Humboldt Universitaet zu Berlin, Berlin, Germany; July 25, 2016.
4. "Nonlinear dynamics induced anomalous Hall effect in topological insulators," Invited talk, 4th International Conference on Application of Nonlinear Dynamics,Denver, Colorado; August 29, 2016.
5. "Multistability in nanosystems," Invited talk, International Seminar and Workshop on Multistability and Tipping: from Mathematics and Physics to Climate and Brain, Max-Planck Institute for Physics of Complex Systems, Dresden, Germany; October 7, 2016.
6. "Relativistic quantum chaos," Plenary talk, 9th Dynamics Days Asia Pacific (DDAP9) - International Conference on Dynamical Systems, Hong Kong Baptist University, Hong Kong; December 14, 2016.

6 Past Honors

1. NSF Faculty Career Award, 1997.
2. Air Force PECASE, 1997.
3. Election as a Fellow of the American Physical Society, 1999. Citation: *For his many contributions to the fundamentals of nonlinear dynamics and chaos*.
4. Outstanding Referee Award, American Physical Society, 2008.
5. Vannevar Bush Faculty Fellow (formerly known as NSSEFF - National Security Science and Engineering Faculty Fellow), Class of 2016. Sponsored by the Basic Research Office of the Assistant Secretary of Defense for Research and Engineering.

AFOSR Deliverables Submission Survey

Response ID:7658 Data

1.

Report Type

Final Report

Primary Contact Email

Contact email if there is a problem with the report.

Ying-Cheng.Lai@asu.edu

Primary Contact Phone Number

Contact phone number if there is a problem with the report

4809656668

Organization / Institution name

Arizona State University

Grant/Contract Title

The full title of the funded effort.

Superpersistent Currents in Dirac Fermion Systems

Grant/Contract Number

AFOSR assigned control number. It must begin with "FA9550" or "F49620" or "FA2386".

FA9550-15-1-0151

Principal Investigator Name

The full name of the principal investigator on the grant or contract.

Ying-Cheng Lai

Program Officer

The AFOSR Program Officer currently assigned to the award

Dr. Arje Nachman

Reporting Period Start Date

06/01/2015

Reporting Period End Date

11/30/2016

Abstract

The principal Objective of the project was to uncover, understand, and exploit persistent currents in 2D Dirac material systems and pertinent phenomena in the emerging field of relativistic quantum nonlinear dynamics and chaos. Systematic theories and methods were developed to analyze and characterize persistent currents in these systems and their unusual physical properties. The main accomplishments are the following: (1) a physical understanding of conductance stability in chaotic and integrable graphene quantum dots with random impurities, (2) the analysis of conductance fluctuations in chaotic bilayer graphene quantum dots, (3) the identification of reverse Stark effect, anomalous optical transitions, and spin control in topological insulator quantum dots, (4) the discovery of nonlinear dynamics induced anomalous Hall effect in topological insulators, (5) the finding that chaos can enhance spin polarization in graphene, (6) the articulation of a robust relativistic quantum two-level system, (7) the discovery and understanding of a number of novel and unusual phenomena associated

with scattering of pesudospin-1 particles, (8) a proposal to resolve the paradox of breakdown of quantum-classical correspondence in optomechanics, (9) the detection of unusual level statistics in graphene billiards, (10) the unearthing of the phenomenon of superscattering of pseudospin-1 wave in a photonic lattice system, (11) the revelation of relativistic Zitterbewegung in non-Hermitian photonic systems, and (12) the elucidation of the robustness of persistent currents in two-dimensional Dirac systems in the presence of random disorders. In addition, the phenomenon of magnetic field induced flow reversal in a ferrofluidic Taylor-Couette system was uncovered, and the issues of multistability, chaos, and random signal generation in semiconductor super lattice systems were addressed.

The AFOSR support provided the opportunity to investigate a number of forefront problems beyond the original proposed research. In addition, the support helped create a new field of interdisciplinary
research: Relativistic Quantum Nonlinear Dynamics and Chaos, which studies the relativistic
quantum manifestations of classical chaos with applications to graphene and two-dimensional Dirac material systems.

The AFOSR project resulted in 17 refereed-journal papers and two PhD dissertations. A new collaboration with AFRL in the areas of semiconductor superlattice and many body effects in pseudo spin-1 Dirac material systems was initiated. A half dozen plenary lectures and invited talks on topics derived from the project were delivered.

Distribution Statement
This is block 12 on the SF298 form.

Distribution A - Approved for Public Release

Explanation for Distribution Statement
If this is not approved for public release, please provide a short explanation. E.g., contains proprietary information.

SF298 Form
Please attach your SF298 form. A blank SF298 can be found here. Please do not password protect or secure the PDF The maximum file size for an SF298 is 50MB.

SF298_FA9550-15-1-0151.pdf

Upload the Report Document. File must be a PDF. Please do not password protect or secure the PDF . The maximum file size for the Report Document is 50MB.

FA9550-15-1-0151-Final_Report_022217.pdf

Upload a Report Document, if any. The maximum file size for the Report Document is 50MB.

Archival Publications (published) during reporting period:

1. G.-L. Wang, L. Ying, and Y.-C. Lai,
"Conductance stability in chaotic and integrable quantum dots with random impurities," Physical Review E 92, 022901, 1-10 (2015).

2. R. Bao, L. Huang, Y.-C. Lai, and C. Grebogi,
"Conductance fluctuations in chaotic bilayer graphene quantum dots," Physical Review E 92, 012918, 1-8 (2015).

3. H.-Y. Xu and Y.-C. Lai, "Reverse Stark effect, anomalous optical transitions, and control of spin in topological insulator quantum dots," Physical Review B 92, 195120, 1-6 (2015).

4. S. Altmeyer, Y.-H. Do, and Y.-C. Lai,
"Ring bursting behavior en route to turbulence in narrow gap Taylor-Couette flows," Physical Review E 92, 053018, 1-10 (2015).

5. S. Altmeyer, Y.-H. Do, and Y.-C. Lai, "Magnetic field induced flow reversal in a ferrofluidic Taylor-Couette system," Scientific Reports 5, 18589, 1-13 (2015).

6. G.-L. Wang, H.-Y. Xu, and Y.-C. Lai, "Nonlinear dynamics induced anomalous Hall effect in topological insulators," Scientific Reports 6, 19803, 1-9 (2016).

7. L. Ying and Y.-C. Lai, "Enhancement of spin polarization by chaos in graphene quantum dot systems," Physical Review B 93, 085408, 1-8 (2016).

8. L. Ying, D.-H. Huang, and Y.-C. Lai, "Multistability, chaos, and random signal generation in semiconductor superlattices," Physical Review E 93, 062204, 1-9 (2016).

9. M.-K. Xu, Y.-S. Wang, R. Bao, L. Huang, and Y.-C. Lai, "Complex transport behaviors of graphene quantum dots subject to mechanical vibrations," Europhysics Letters 114, 47006, 1-6 (2016).

10. H.-Y. Xu, L. Huang, and Y.-C. Lai, "A robust relativistic quantum two-level system with edge-dependent currents and spin polarization,"
Europhysics Letter 115, 20005, 1-7 (2016).

11. H.-Y. Xu and Y.-C. Lai, "Revival resonant scattering, perfect caustics and isotropic transport of pesudospin-1 particles," Physical Review B 94, 165405, 1-16 (2016).

12. G.-L. Wang, Y.-C. Lai, and C. Grebogi, "Transient chaos: breakdown of quantum-classical correspondence in optomechanics," Scientific Reports 6, 35381, 1-13 (2016).

13. P. Yu, Z.-Y. Li, H.-Y. Xu, L. Huang, B. Dietz, C. Grebogi, and Y.-C. Lai, "Gaussian orthogonal ensemble statistics in graphene billiards with the shape of classically integrable billiards," Physical Review E 94, 062214, 1-12 (2016).

14. H.-Y. Xu and Y.-C. Lai, "Superscattering of pseudospin-1 wave in photonic lattice," Physical Review A 95, 012119, 1-7 (2017).

15. S. Altmeyer, Y.-H. Do, and Y.-C. Lai, "Dynamics of ferrofluidic flow in small aspect-ratio Taylor-Couette systems," Scientific Reports 7, 40012, 1-19 (2017).

16. G.-L. Wang, H.-Y. Xu, L. Huang, and Y.-C. Lai,
"Relativistic Zitterbewegung in non-Hermitian quantum photonic waveguide systems," New Journal of Physics, in press
.
17. L. Ying and Y.-C. Lai, "Robustness of persistent currents in two-dimensional Dirac systems with disorders," Physical Review B, revised.

New discoveries, inventions, or patent disclosures:

Do you have any discoveries, inventions, or patent disclosures to report for this period?

No

Please describe and include any notable dates

Do you plan to pursue a claim for personal or organizational intellectual property?

Changes in research objectives (if any):

None

Change in AFOSR Program Officer, if any:

None

Extensions granted or milestones slipped, if any:

None

AFOSR LRIR Number

LRIR Title

Reporting Period

Laboratory Task Manager

Program Officer

Research Objectives

Technical Summary

Funding Summary by Cost Category (by FY, $K)

	Starting FY	FY+1	FY+2
Salary			
Equipment/Facilities			
Supplies			
Total			

Report Document

Report Document - Text Analysis

Report Document - Text Analysis

Appendix Documents

2. Thank You

E-mail user

Feb 22, 2017 16:12:37 Success: Email Sent to: Ying-Cheng.Lai@asu.edu